# Asymptotic Performance of M-ary Signals on Rician Fading Diversity Channels

by

Hongwei Zhang

A thesis

presented to Lakehead University

in fulfillment of the

thesis requirement for the degree of

Master of Science in Engineering

in

Control Engineering

Thunder Bay, Ontario, Canada, 2007

© Hongwei Zhang 2007

# Canada

# Asymptotic Performance of M-ary Signals on Rician Fading Diversity Channels

by

Hongwei Zhang

Submitted to the Department of Electrical Engineering
in September 2007, in partial fulfillment of the
requirements for the degree of
Master of Science

**Abstract**

In this thesis, we will study the average symbol error rate of M-ary signals on wireless Rician fading channels at high average signal-to-noise ratio (SNR) in both single-carrier and multicarrier orthogonal frequency division multiplexing (OFDM) systems. In the system discussed, diversity reception with maximal ratio combining (MRC) and equal gain combining (EGC) is adopted. A general theorem relates the asymptotic error rate to the multidimensional integral of the conditional error probability is presented. Two other theorems are presented for the special cases where the conditional error probability is function of the sum of received SNR's and the sum of received amplitudes corresponding to the cases using MRC diversity and EGC diversity respectively. Then theorems are provided to analyze the asymptotic error rate performance of M-ary signlas including M-ary phase-shift keying (MPSK), M-ary pulse amplitude modulation (MPAM), and M-ary quadrature amplitude modulation (MQAM) signals in both single-carrier and multicarrier OFDM systems.

Thesis Supervisor: Zhiwei Mao
Title: Assistant Professor, Electrical Engineering

# Contents

# List of Figures

# List of Tables

# Chapter 1

# Introduction

The elements of communication system are the transmitter, the channel, and the receiver. Modulated information signals are transmitted through the channel to reach the receiver, where the received signals are demodulated. The channels considered in this thesis are wireless Rician fading channels. At the receiver, diversity technique is used to mitigate the fading effects.

In mobile radio channels, Rayleigh distribution is widely used to represent the statistical characteristics of the received signal envelope of a fading channel, or the received envelope of an individual multipath component. When there is a dominant stationary signal component present, such as a line-of-sight (LOS) propagation path, the received signal envelope of a fading channel or an individual multipath component follows Rician distribution.

It is observed that even when one radio path undergoes a deep fade, another independent path may not and may have a strong signal power at the same instance of time. By having multiple independent paths to choose from or to combine, both the instantaneous and the average signal-to-noise ratios (SNRs) at the receiver may be improved, by as much as 20 to 30 dB. Diversity technique is based on this observation and is a useful receiver technique in wireless communication systems.

7

Orthogonal frequency-division multiplexing (OFDM) is a promising technique to combat ISI due to frequency selective multipath propagation of the channel. In OFDM, the wideband channel is divided into a number of orthogonal subchannels with equal bandwidth which is sufficiently narrow so that the frequency response characteristics of each subchannel are nearly flat.

Symbol error rate is a measure of the performance of communication system. In this thesis, the error rate performance of M-ary signals on Rician fading diversity channels will be studied. However, the exact error rate expressions are too complex. Therefore, asymptotic error rate at high average SNR will be considered. A general theorem will be proved to relate the asymptotic error rate to the multidimensional integral of the conditional error probability [1]. Two other theorems will be presented for the special cases where the conditional error probability is function of the sum of received SNR's and the sum of received amplitudes, respectively [1]. Then theorems are provided to analyze the asymptotic error rate of M-ary signals including M-ary phase-shift keying (MPSK), M-ary pulse amplitude modulation (MPAM), M-ary quadrature amplitude modulation (MQAM), M-ary frequency shift keying (MFSK) in single-carrier systems. The discussion is also extended to OFDM systems. Results obtained in this thesis could be used to assist the design and control of wireless communication systems. Some examples may include transmission scheme selection, transmission power control, receiver diversity control, etc.

The thesis derives some new results of asymptotic performance on MQAM and

8

other signallings and extend them to OFDM systems.

The remaining parts of this thesis are organized as follows. In Chapter 2, basic concepts used in the thesis will be introduced, which include M-ary digital modulation, symbol error rate (SER) performance of M-ary signaling, fading channel, diversity, and OFDM. The asymptotic performance of single-carrier and OFDM M-ary signals on multipath Rician fading diversity channels will be discussed in Chapters 3 and 4, respectively. Chapter 5 presents conclusions and some topics for future study.

9

# Chapter 2

# Some Fundamentals

In this chapter, we will give some basic concepts used in the thesis. They are

M-ary digital modulation, multipath fading channel, diversity technique and OFDM.

First, we introduce the basic concept of M-ary digital modulation, which includes

MPAM, MFSK, MPSK, and MQAM. Then, we introduce fading channel, including

flat fading channel and frequency selective fading channel. Diversity technique is then

discussed. Finally, some fundamentals about OFDM are discussed.

## 2.1 M-ary Digital Modulation

In digital modulation, digital information is transmitted through a

communication channel by mapping it into analog waveforms of the form [2]

$$s(t) = A_c \cos(2\pi f_c t + \phi_c) \qquad 0 \le t \le T \qquad (2.1)$$

where $A_c$ is the carrier amplitude, $f_c$ is the carrier frequency, $\phi_c$ is the carrier

phase, and $T$ is the symbol interval.

In M-ary digital modulation, blocks of $\log_2 M$ binary digits from information

message are taken at a time and mapped into one of the $M$ waveforms

$\{s_m(t), m = 1,2,...,M\}$ for transmission over the channel. These $M$ waveforms may

differ in amplitude, or frequency, or phase, or some combination of the parameters,

which correspond to MPAM, MFSK, MPSK, and MQAM, respectively. In the

10

following, more detailed discussion will be included on each of the modulation

schemes.

**M-ary Phase-Shift Keying (MPSK) Signaling**
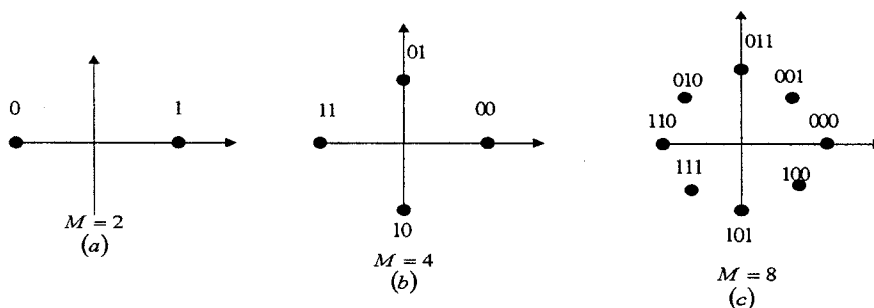


Figure 2.1 Signal space diagrams for PSK signal

In MPSK, the transmitted signal can be represented as

$$s_m(t) = A_c \cos(2\pi f_c t + \phi_{c,m}) \quad m = 1,...,M; 0 \le t \le T \tag{2.2}$$

where $\left\{ \phi_{c,m}(t) = \dfrac{2\pi}{M}(m-1), m = 1,2,...,M \right\}$ denote the $M$ possible carrier phases

representing the information.

Assume Gray coding, the corresponding signal space diagrams for

$M = 2$, $M = 4$ and $M = 8$ are given in Figure 2.1 [3]. For example, for the case of

$M = 2$, the zero degree phase represents the transmitted information '1', while the

180 degree phase represents the transmitted information '0'. It is noted that all

constellations are equally spaced on a circle for MPSK signaling.

11

## M-ary Pulse Amplitude Modulation (MPAM) Signaling
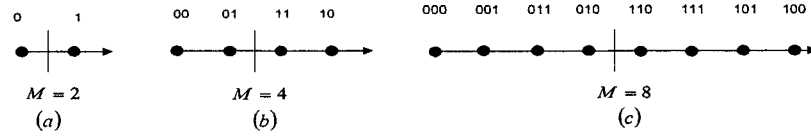


Figure 2.2 Signal space diagrams for PAM signal

In MPAM, the transmitted signal can be represented as

$$s_m(t) = A_{c,m} \cos(2\pi f_c t + \phi_c) \qquad m = 1,...,M; 0 \le t \le T \qquad (2.3)$$

where $\{A_{c,m}, m = 1,2,...,M\}$ denote the $M$ possible amplitudes representing the $M$

different possible $\log_2 M$ -bit information blocks.

Assume Gray coding, the corresponding signal space diagrams

for $M = 2$, $M = 4$ and $M = 8$ are given in Figure 2.2 [3]. It is noted from Figure

2.1 and 2.2 that the dimensionality of the signal space for MPAM signals is only one,

while that for MPSK signal is two.

## M-ary Frequency-Shift Keying (MFSK) Signaling

In MFSK, the transmitted signal can be represented as

$$s_m(t) = A_c \cos(2\pi f_{c,m} t + \phi_c) \qquad m = 1,...,M; 0 \le t \le T \qquad (2.4)$$

where $\{f_{c,m}(t) = f_c + m\Delta f, m = 1,2,...,M\}$ denote the $M$ possible carrier

frequencies representing the information. It is noted that in order to keep the

orthogonality of the $M$ signals, the minimal frequency separation between adjacent

signals is $\Delta f = \dfrac{1}{2T}$ [2].

12

# M-ary Quadrature Amplitude Modulation (MQAM) Signaling
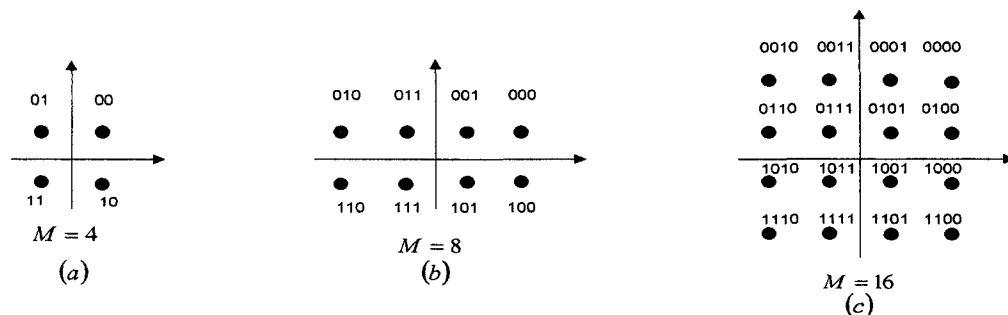


Figure 2.3 Signal space diagrams for rectangular QAM signals

In MQAM, the transmitted signal can be represented as

$$s_m(t) = A_{c,m} \cos\left(2\pi f_c t + \phi_{c,m}\right) \qquad m = 1,...,M; 0 \le t \le T. \tag{2.5}$$

From (2.5), it can be seen that MQAM may be considered as a combination of amplitude and phase modulations. MQAM signals can be constructed by impressing separate information bits onto two quadrature carriers, $\cos 2\pi f_c t$ and $\sin 2\pi f_c t$ using PAM. Assume Gray coding, examples of signal space diagrams for $M = 4$, $M = 8$ and $M = 16$ are given in Figure 2.3.

## 2.2 Symbol Error Rate (SER) Performance of M-ary Signaling in AWGN Channels

Assuming that the M-ary signal is transmitted through an additive white Gaussian noise (AWGN) channel, the received signal can be expressed as

$$r(t) = s_m(t) + n(t) \qquad 0 \le t \le T \quad m = 1,...M \tag{2.6}$$

where $n(t)$ denotes the AWGN process. Based on $r(t)$, a decision is made regarding which of the M possible waveforms was transmitted. In the following, we will discuss the probability of making a symbol decision error for different M-ary

13

signaling schemes [3] .

### MPSK Signaling

The SER of MPSK with coherent receiver is given as [3]

$$p_e(\xi;M) \approx 2Q\left(\sqrt{2\xi}\sin\frac{\pi}{M}\right) = erfc\left(\sqrt{\xi}\sin\frac{\pi}{M}\right) \qquad (2.7)$$

where $\xi$ denotes the SNR of the decision variable, $\quad Q(y) = \int_y^\infty \frac{1}{\sqrt{2\pi}} e^{-t^2/2} dt$ ,

$y \geq 0 \quad erfc(y) = \frac{2}{\sqrt{\pi}} \int_y^\infty e^{-t^2} dt, y \geq 0$ and it is noticed that $Q(y) = \frac{1}{2} erfc\left(\frac{y}{\sqrt{2}}\right)$ .

In "A new simple and exact result for calculating the probability of error for two-dimensional signal constellations", the SER of MPSK is also proved to be [4]

$$p_e(\xi;M) = \frac{1}{\pi} \int_{\pi/M}^\pi d\theta \exp\left[-\xi\frac{\sin^2(\pi/M)}{\sin^2\theta}\right] . \qquad (2.8)$$

### MPAM Signaling

The SER of MPAM with coherent receiver is given as [3]

$$p_e(\xi;M) = \frac{2(M-1)}{M}Q\left(\sqrt{\frac{6\xi}{(M^2-1)}}\right)$$

$$= \frac{M-1}{M} erfc\left(\sqrt{\frac{3\xi}{(M^2-1)}}\right). \qquad (2.9)$$

### MFSK Signaling

The SER of MFSK with noncoherent receiver is given as [1]

$$p_e(\xi;M) = \sum_{m=1}^{M-1} \frac{(-1)^{m+1}}{m+1}\binom{M-1}{m}\exp\left[\frac{-m\xi}{m+1}\right] . \qquad (2.10)$$

Whereas the SER of MFSK with coherent receiver is given as [1]

$$p_e(\xi,M) = \frac{1}{\sqrt{\pi}} \int_{-\infty}^\infty \left[1 - \left(\frac{1}{2}erfc(-y)\right)^{M-1}\right]\exp\left[-\left(y-\sqrt{\xi}\right)^2\right]dy. \qquad (2.11)$$

### MQAM Signaling

14

The SER of MQAM is given as [3]

$$p_e(\xi;M) = 4\left(1-\frac{1}{\sqrt{M}}\right)Q\left(\sqrt{\frac{3\xi}{(M-1)}}\right) - 4\left(1+\frac{1}{M}-\frac{2}{\sqrt{M}}\right)Q^2\left(\sqrt{\frac{3\xi}{(M-1)}}\right). \quad (2.12)$$

It is noted that, the SER performance of 4-QAM and 4-PSK is approximated identical.

Using (2.7), the SER of 4-PSK is $p_e(\xi;4) \approx 2Q\left(\sqrt{\xi}\right)$ . On the other hand, Using

(2.12), the SER of 4-QAM is $p_e(\xi;4) = 2Q\left(\sqrt{\xi}\right) - Q^2\left(\sqrt{\xi}\right) \approx 2Q\left(\sqrt{\xi}\right)$. These results

show the correctness of (2.7) and (2.12).

## 2.3 Fading Channel
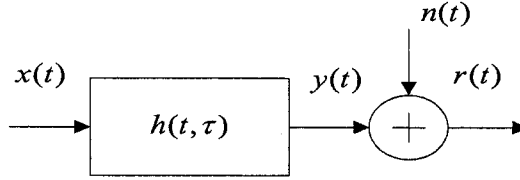


Figure 2.4 Equivalent complex baseband channel model

An equivalent model for a complex time varying communication channel is

given in Figure 2.4 [1]. It is shown that the received signal $r(t)$ can be expressed as

$$r(t) = x(t) \otimes h(t,\tau) + n(t) \quad (2.13)$$

where $\otimes$ represents convolution, $x(t)$ denotes the transmitted signal, $h(t,\tau)$

represents the impulse response of the channel, and $n(t)$ is the noise. The impulse

response $h(t,\tau)$ completely characterizes the channel and is a function of both $t$

and $\tau$. The variable $t$ represents the time variations due to motion, whereas $\tau$

represents the channel multipath delay for a fixed value of $t$ [5].
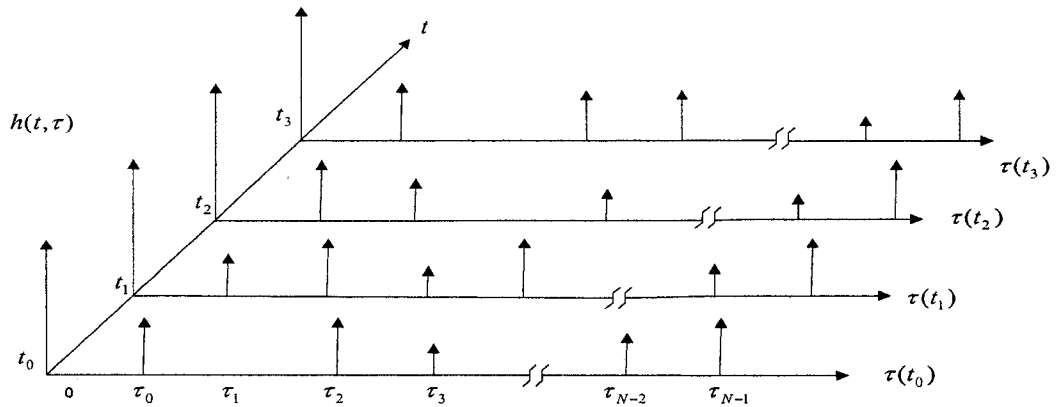
Figure 2.5 An example of discrete-time impulse response model for a time varying multipath radio channel

In wireless communication systems, especially wireless mobile communication systems, the receiver may receive multiple versions of the same transmitted signal at slightly different times due to the slightly different distances thus different excess delays of different paths. Those paths may include the shortest line-of-sight (LOS) path, the reflection paths which are produced from surfaces much larger than the signal wavelength, the diffraction paths which are produced at the sharp edge of an impenetrable body with dimension larger than the signal wavelength, and the scattering paths which are produced when the transmitted signal hits on large number of rough objects with small size compared to the signal wavelength. Therefore the complex impulse response for a general time varying multipath radio channel can be given as [6]

$$h(t,\tau) = \sum_{k=0}^{K-1} \alpha_k(t)\delta[\tau - \tau_k(t)] \qquad (2.14)$$

where $K$ represents the number of possible multipath components, $\alpha_k(t)$ and $\tau_k(t)$ are the complex gain and excess delay of the $k$ th multipath component at time $t$.

16

Figure 2.5 [5] shows an example of discrete-time impulse response model for a time varying multipath radio channel.

Based on the multipath delay spread, we define a channel parameter of channel coherence bandwidth $(B_c)$, which is given as [5]

$$B_c \approx \frac{1}{c\delta_\tau} \qquad (2.15)$$

where $\delta_\tau$ is the rms delay spread defined as [5]

$$\delta_\tau = \sqrt{\overline{\tau^2} - \left(\overline{\tau}\right)^2} \; . \qquad (2.16)$$

With $\overline{\tau}$ being the mean excess delay and $\overline{\tau^2}$ being the second moment of the excess delay. $c$ is a constant that depends on the frequency correlation function requirement in the definition of $B_c$. For instance, if the frequency correlation function is at least 0.9, $c = 50$, whereas if the frequency correlation function is at least 0.5, $c = 5$. Accordingly, radio channels can be classified into flat fading or frequency selective fading channels.

**Flat Fading Channel**
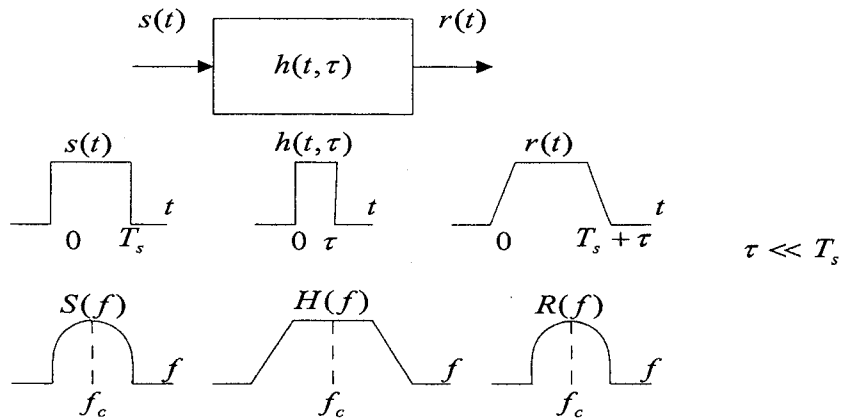


Figure 2.6 Flat fading channel characteristics

17

If the transmitted signal has a bandwidth $W < B_c$, the channel is called flat

fading channel. In flat fading channels, all frequency components in the transmitted

signal undergo the same gain and linear phase response. The characteristics of a flat

fading channel are illustrated in Figure 2.6 [5]. Therefore, flat fading channels are also

referred to as narrowband channels. It can be seen that in flat fading channels,

although the received signal may undergo amplitude fluctuations due to the variation

in the channel gain over time, the spectral characteristics of the transmitted signal is

kept in the received signal.

**Frequency Selective Fading Channel**
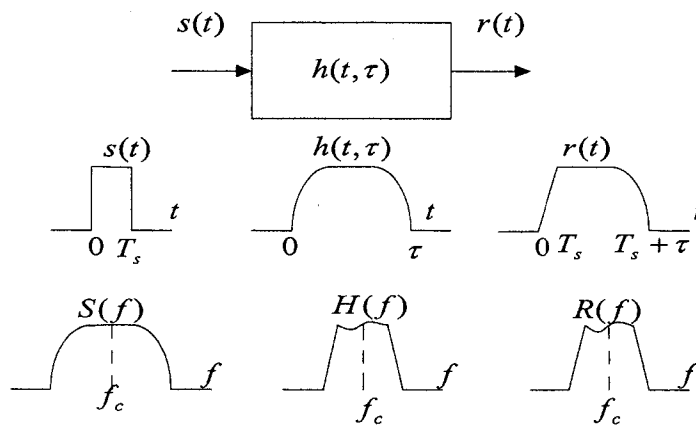


Figure 2.7 Frequency selective fading channel characteristics

If the transmitted signal has a bandwidth $W > B_c$, the channel is called

frequency selective. Frequency selective fading channels are also known as wideband

channels. Frequency selective fading is caused by multipath delays which approach or

exceed the symbol period of the transmitted symbol. The characteristics of a

frequency selective fading channel are illustrated in Figure 2.7 [5]. It can be seen that

18

in frequency selective fading channels, channel gains and phase responses vary over the spectrum of the transmitted signal and the received signal is distorted and time-dispersed. Due to the time dispersion, transmitted symbols may overlap with each other and thus inter-symbol interference (ISI) is induced.

**Rayleigh and Rician Fading**

The envelope of the sum of two independent quadrature Gaussian random signals with zero mean and common variance obeys a Rayleigh distribution. That is, let

$$R = \sqrt{X_1^2 + X_2^2} \qquad (2.17)$$

where $X_1$ and $X_2$ are statistically independent Gaussian random variables with mean $m_1 = m_2 = 0$ and variance $\sigma_1^2 = \sigma_2^2 = \sigma^2$, then $R$ follows Rayleigh distribution with a probability density function (PDF) given by [3]

$$p_R(r) = \frac{r}{\sigma^2} \exp\left(-\frac{r^2}{2\sigma^2}\right), r \geq 0. \qquad (2.18)$$

In mobile radio channels, the Rayleigh distribution is widely used to represent the statistical characteristics of the received signal envelope of a flat fading channel, or the received envelope of an individual multipath component.

When there is a dominant stationary signal component present, such as a LOS propagation path, the received signal envelope of a flat fading channel or an individual multipath component follows Rician distribution, whose PDF is given by [3]

19

$$p_R(r) = \frac{r}{\sigma^2} e^{-(r^2+s^2)/2\sigma^2} I_0\left(\frac{rs}{\sigma^2}\right), s > 0, r > 0 \qquad (2.19)$$

where $s$ denotes the peak amplitude of the dominant signal, $I_0(.)$ is the modified

Bessel function of the first kind and zero-order. It can be seen that if $s = 0$, i.e., if the

dominant path diminishes, a Rician fading reduces to a Rayleigh fading.

## 2.4 Diversity Technique

It is observed that even when one radio path undergoes a deep fade, another

independent path may not and may have a strong signal power at the same instance of

time. By having multiple independent paths to choose or to combine, both the

instantaneous and the average signal-to-noise ratios (SNRs) at the receiver may be

improved, by as much as 20 to 30 dB [5]. Diversity technique is based on this

observation and is a useful receiver technique in wireless communication systems.

The most widely used form of diversity in wireless communication systems is to

use multiple receiving antennas, also called an antenna array, where the elements of

the array are separated enough in distance, often on the order of several tens of

wavelengths. This type of diversity is referred to as space diversity. With space

diversity, independent fading paths are realized without an increase in transmitted

signal power or transmission bandwidth.

Other methods of achieving diversity include polarization diversity, frequency

diversity, and time diversity. In polarization diversity, multiple versions of the

information signal are transmitted via antennas using orthogonal polarizations, like

circular and linear polarizations. In frequency diversity, multiple versions of the

20

information signal are transmitted on multiple carrier frequencies, which are separated by at least the channel coherence bandwidth. In time diversity, information signals are transmitted repeatedly at enough time spacings.

A generalized block diagram for diversity with $M$ independent branches is given in Figure 2.8 [5]. Based on the reception method, diversity techniques can be classified into selection diversity, maximum ratio combining (MRC) diversity, and equal gain combining (EGC) diversity.
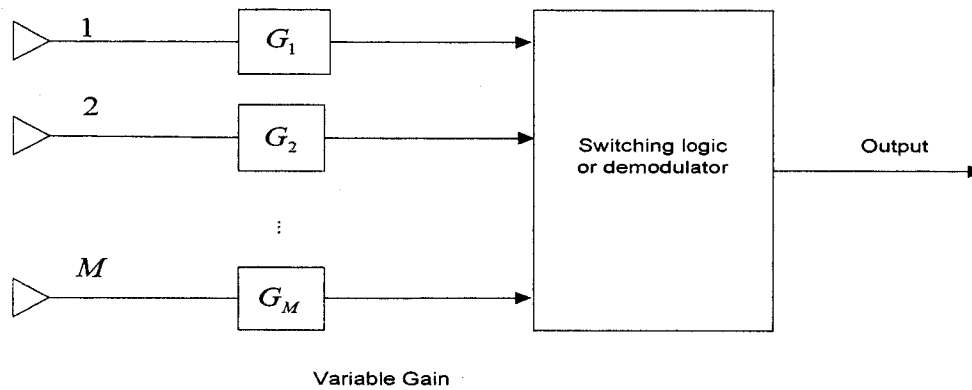
Figure 2.8 Generalized block diagram for diversity

### Selection Diversity

In selection diversity, the receiver branch with the highest instantaneous SNR is connected to the demodulator and provides the output. Selection diversity is easy to implement because all that is needed is a monitoring station and a switch at receiver. However, it is not an optimal diversity technique because it does not use all possible branches simultaneously.

21

**Maximal Ratio Combining (MRC)**
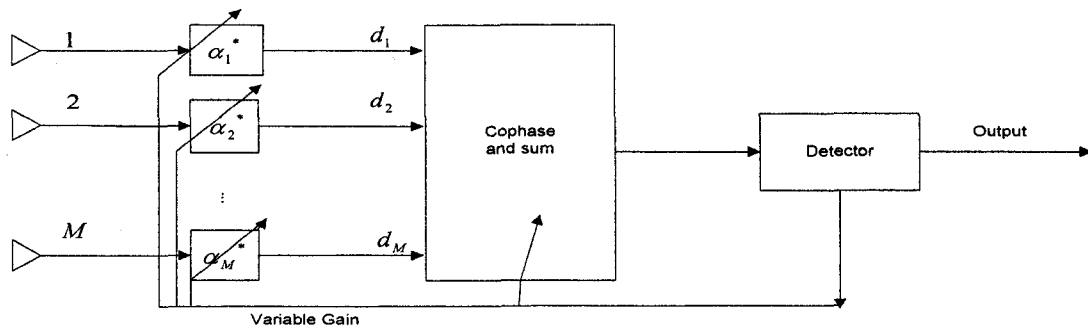


Figure 2.9 Maximum radio combining

In MRC, the signals from all of the $M$ available branches are weighted according to their individual SNRs and then co-phased and summed. MRC uses all of the $M$ available branches in a co-phased and weighted manner such that the output SNR is the sum of the SNRs of all branches, which is the highest achievable SNR at the receiver. A block diagram of MRC is shown in Figure 2.9 [5], in which $\alpha_m^*$ equals to the conjugate of $\alpha_m$ [7] [8].

**Equal Gain Combining (EGC)**

In EGC, the branch weights are all set to unity, but the signals from each branch are co-phased to exploit the signal received from all branches simultaneously. EGC has a much easier implementation than MRC, but its performance is only marginally inferior to that of MRC and much better than that of selection diversity.

22

## 2.5 Orthogonal Frequency-Division Multiplexing (OFDM)
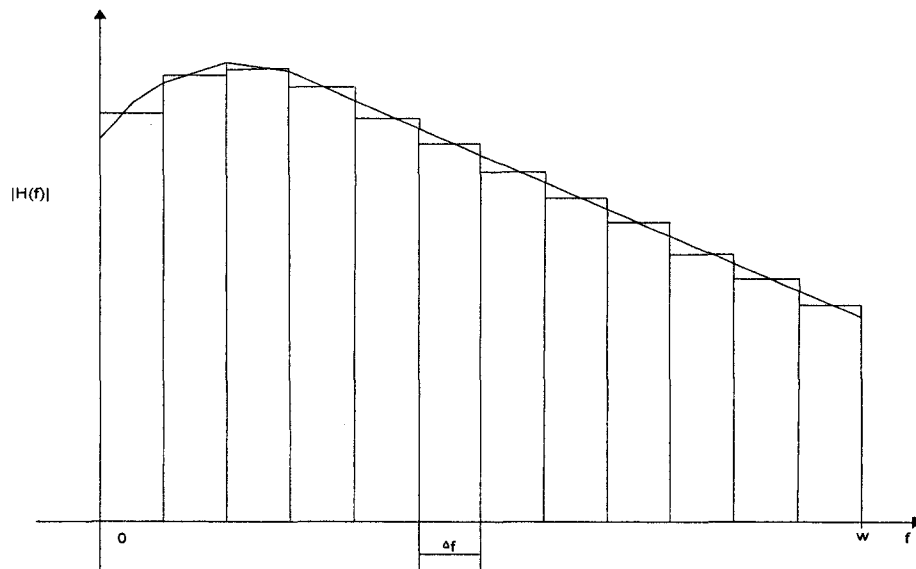


Figure 2.10 Principle of OFDM

As a technique to combat ISI due to frequency selective multipath propagation of channel, OFDM is now widely used in our life. Example applications include wideband data communications over mobile radio FM channel, high-bit-rate digital subscriber lines (HDSL), asymmetric digital subscriber lines (ADSL), very-high-speed digital subscriber lines (VDSL), digital audio broadcasting (DBA) and high-definition television (HDTV) terrestrial broadcasting [9].

OFDM is a promising technique to combat ISI due to frequency selective multipath propagation of the channel. As shown in Figure 2.10 [2] , in OFDM, the wideband channel with bandwidth $W$ is divided into a number of orthogonal subchannels with equal-bandwidth $\Delta f$ which is sufficiently narrow so that the frequency response characteristics of each subchannel are nearly flat.

In Figure 2.11 [10], an OFDM multicarrier transmitter and receiver is given .

23
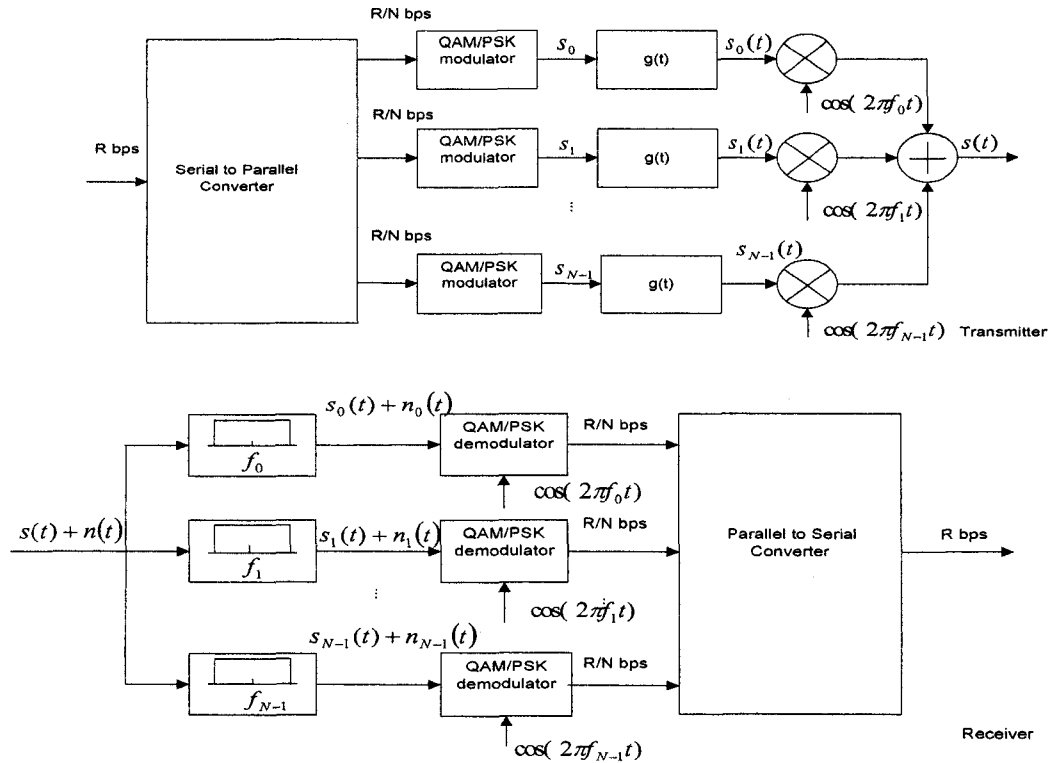
Figure 2.11 OFDM multicarrier transmitter and receiver

We can improve the spectral efficiency of OFDM by overlapping the subchannels. The subcarriers must still be orthogonal so that they can be separated by the receiver. Note that the baseband subcarriers $\{\cos(2\pi jt/T + \phi_j), j = 1,2...\}$ form a set of orthogonal basis functions on the interval $[0,T]$ for any set of subcarrier phase offsets $\{\phi_j\}$. This implies that the minimum frequency separation required for sub-carriers to remain orthogonal over the symbol interval $[0,T]$ is $1/T$ for arbitrary subcarrier phase offsets. So if we use raised cosine pulses

$$g(t) = \frac{\sin \pi t/T}{\pi t/T} \frac{\cos \beta \pi t/T}{1 - 4\beta^2 t^2/T^2} \quad , \tag{2.20}$$

it can be shown that we have

$$T = 0.5(1 + \beta)/B \tag{2.21}$$

24

With $\beta = 1$, we would have $T = 1/B$, and a carrier separation of $B$. Since the passband bandwidth of each subchannel is $2B$, the passband subchannels in this system would overlap. OFDM signal with overlapping subcarriers is shown in Figure 2.12 [10].
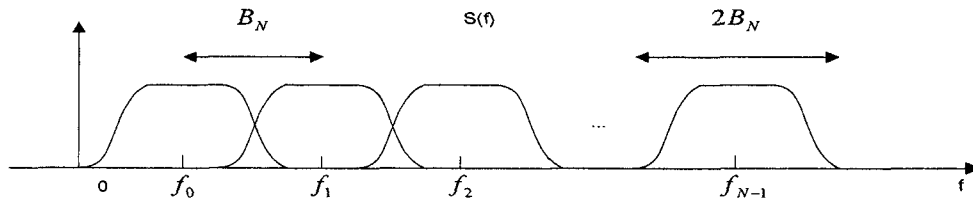


Figure 2.12 OFDM signal with overlapping subcarrier
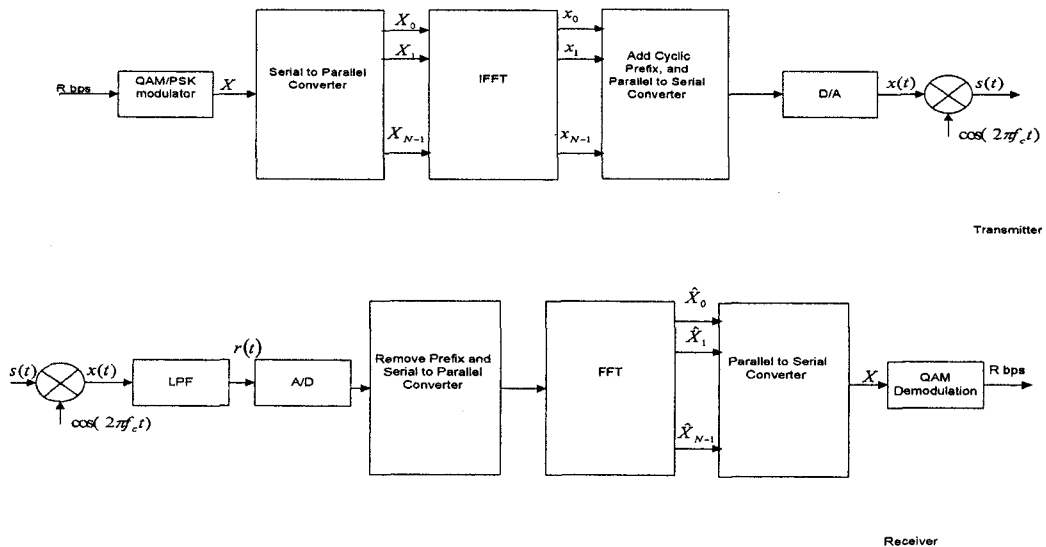


Figure 2.13 OFDM with IFFT/FFT Implementation

An equivalent IFFT/FFT implementation of OFDM is given in Figure 2.13 [10]. At the transmitter, a serial-to-parallel converter divides the input information stream into $N$ substreams, each of which is transmitted over a different subcarrier, implemented using an inverse fast Fourier transform (IFFT). The signal samples $x_n(n = 0,...,N-1)$ generated by computing the IFFT of the input symbols

25

$X_k (k = 0,...,N-1)$ and parallel-to-serial converted, are passed through a digital-to-analog (D/A) converter whose output is the OFDM signal waveform $x(t)$. In order to eliminate the residual ISI, a cyclic prefix is added to each block of the $N$ signal samples.

The received signal is first passed through an analog-to-digital (A/D) converter and becomes a digital signal. Then, the prefix is removed and the remaining part of the digital signal is passed through a serial-to-parallel converter and becomes N parallel digital signals. The signal $\hat{X}_n (n = 0,...,N-1)$ generated by computing the FFT of the N parallel digital signals is then passed through a parallel-to-serial converter and demodulated to provide a recovered version of the information stream.

26

# Chapter 3

# Asymptotic Performance of Single-Carrier M-ary Signals on Multipath Rician Fading Diversity Channels

In this chapter, we consider the performance of digital communication systems with single-carrier M-ary signals on multipath Rician fading diversity channels. The exact error rate is so complex that we consider the asymptotic error rate at high average SNRs. A general theorem is provided to reveal the asymptotic error probability of single-carrier signals over multipath Rician fading channels. Another two theorems are also studied for the special cases in which the conditional error probability is a function of the sum of the received signal SNRs in multipaths or a function of the sum of the received signal amplitudes in multipaths. We derive closed-form asymptotic error expressions for single-carrier digital communication systems with MPSK, MPAM, MQAM, and MFSK signalings.

## 3.1 System Model
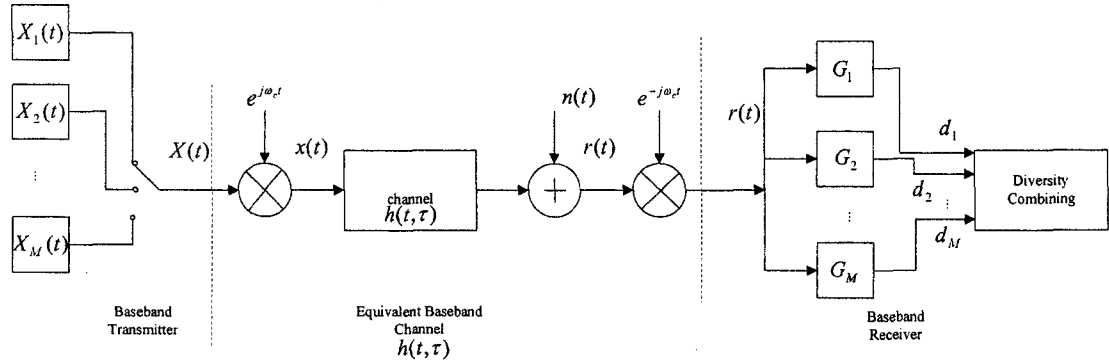


Figure 3.1 Communication system

The system considered in this chapter is given in Figure 3.1. The transmitter sends one of the $M$ possible signals. We assume that $E$ is the average transmitted energy per symbol. As given in (2.14), the complex impulse response for a multipath channel is given as

$$h(t,\tau) = \sum_{k=0}^{K-1} \alpha_k(t)\delta[\tau - \tau_k(t)] \; . \tag{3.1}$$

It is assumed that the fading is slow, i.e., over the period of a symbol duration $T$, the channel keeps constant. Therefore, (3.1) can be simplified as

$$h(t,\tau) = \sum_{k=0}^{K-1} \alpha_k \delta[\tau - \tau_k] \tag{3.2}$$

where $\alpha_k$ can be given as $\alpha_k = a_k e^{j\theta_k}$.

We assume that the amplitudes of the received $k$ th path $a_k$ for $k = 1,...,K$ are independent and each follows a Rician distribution, that is, the PDF of $a_k$ is given as

[1]

28

$$f(a_k) = \frac{a_k}{\sigma_k^2} \exp\left[-\frac{v_k^2 + a_k^2}{2\sigma_k^2}\right] I_0\left(\frac{a_k v_k}{\sigma_k^2}\right) \qquad (3.3)$$

where $v_k$ is the nonfading signal component or dominant (specular) component, $2\sigma_k^2$ is average power in the random component.

It can be shown that the PDF of $\rho_k = a_k^2 E / N_0$ is given by [1]

$$f(\rho_k) = \frac{1}{\gamma_k} \exp\left[-\frac{P_k + \rho_k}{\gamma_k}\right] I_0\left(\frac{2\sqrt{\rho_k P_k}}{\gamma_k}\right) \qquad (3.4)$$

where $N_0 / 2$ is additive white Gaussian noise power spectral density. $P_k = v_k^2 E / N_0$ is the SNR of the dominant component, $\gamma_k = 2\sigma_k^2 E / N_0$ is the average SNR of the random component. The parameters $\delta_k = \dfrac{P_k}{\gamma_k} = \dfrac{v_k^2}{2\sigma_k^2}$ also known as Rician K factor

and $\Delta_k = \sum\limits_{k=0}^{K-1} \delta_k$ are of importance in evaluating the performance in Rician fading channels. Therefore, $f(\rho_k)$ can also be given as [1]

$$f(\rho_k) = \frac{1}{\gamma_k} e^{-\delta_k} e^{-\frac{\rho_k}{\gamma_k}} I_0\left(2\sqrt{\frac{\delta_k \rho_k}{\gamma_k}}\right) . \qquad (3.5)$$

We denote the symbol error rate conditioned on the value of $\rho$ , which is called conditional SER.

$$p_e(\rho; M) = p_e(\rho_0, \ldots, \rho_{K-1}; M) . \qquad (3.6)$$

where $M$ stand for M-ary.

Due to the independency of multiple paths, which is a reasonable and widely used assumption, the elements of $\rho$ are independent. Therefore, the joint PDF $f(\rho)$ is given as

$$f(\rho) = f(\rho_0) f(\rho_1) \ldots f(\rho_{K-1}). \qquad (3.7)$$

29

The average SER over the Rician channel can therefore be obtained by averaging the conditional SER over the PDF of $f(\rho)$, that is [1]

$$P_e(K;M) = \frac{e^{-\Delta_K}}{\Gamma_{K,M}} \int_0^\infty \cdots \int_0^\infty \prod_{k=0}^{K-1} \left[ e^{-\frac{\rho_k}{\gamma_k}} I_0\left(2\sqrt{\frac{\delta_k \rho_k}{\gamma_k}}\right) \right] p_e(\rho_0,...,\rho_{K-1};M) d\rho_0...d\rho_{K-1} \quad (3.8)$$

where $\Gamma_{K,M} = \prod_{k=0}^{K-1} \gamma_k$. Note that the SER discussed in chapter 2 is conditional SER.

The asymptotic value of $P_e(K;M)$ with $\gamma_k \gg 1, \forall k$ is [1]

$$P_{e_{asy}}(K;M) = \frac{e^{-\Delta_k} \lambda_{K,M}}{\Gamma_{K,M}} \quad (3.9)$$

where $\lambda_{K,M}$ is a symbol asymptotic parameter defined as [1]

$$\lambda_{K,M} = \lim_{\gamma_0...\gamma_{K-1} \to \infty} [\Gamma_{K,M} e^{\Delta_k} P_e(K;M)]. \quad (3.10)$$

We also define $\lambda_{b_K,M}$ as [1]

$$\lambda_{b_K,M} = \frac{\lambda_{K,M}}{(\log_2 M)^K}. \quad (3.11)$$

$\lambda_{b_K,M}$ is the symbol asymptotic parameter relative to the average bit SNR.

## 3.2 A General Asymptotic Theorem

Theorem 1[1] : If $p_e(\rho;M)$ is integrable in the K-dimensional space of $\rho$ and if the integral $\int_0^\infty \rho_k^\alpha p_e(\rho_0,...,\rho_{K-1};M) d\rho_k, 0 \le k \le K-1$ results in a singularity of order less than $\alpha, \forall \alpha > 0$, then $\lambda_{K,M}$ is equal to the volume enclosed by $p_e(\rho;M)$ in the K-dimensional space, that is

$$\lambda_{K,M} = \int_0^\infty \cdots \int_0^\infty p_e(\rho_0,...,\rho_{K-1};M) d\rho_0...d\rho_{K-1} \quad (3.12)$$

Proof:

We start the proof of Theorem 1 by considering the single path channel. For $K = 1$

30

$$P_e(1;M) = \frac{e^{-\delta_0}}{\gamma_0} \int_0^\infty e^{-\frac{\rho_0}{\gamma_0}} I_0\left(2\sqrt{\frac{\delta_0 \rho_0}{\gamma_0}}\right) p_e(\rho_0;M) d\rho_0.$$

By using the trigonometric form of $I_0(x) = \frac{1}{\pi} \int_0^\pi d\theta \cos\theta e^{x\cos\theta}$, $P_e(1;M)$ can be given as

$$P_e(1;M) = \frac{e^{-\delta_0}}{\gamma_0} \int_0^\infty d\rho_0 e^{-\frac{\rho_0}{\gamma_0}} p_e(\rho_0;M) \frac{1}{\pi} \int_0^\pi d\theta \cos\theta e^{2\sqrt{\frac{\delta_0 \rho_0}{\gamma_0}} \cos\theta}.$$

Therefore,

$$\gamma_0 e^{\delta_0} P_e(1;M) = \frac{1}{\pi} \int_0^\pi d\theta \int_0^\infty d\rho_0 e^{-\frac{\rho_0}{\gamma_0}} e^{2\sqrt{\delta_0} \cos\theta \sqrt{\frac{\rho_0}{\gamma_0}}} p_e(\rho_0;M).$$

By expanding the two exponents using Taylor series expansion, we obtain

$$\gamma_0 e^{\delta_0} P_e(1;M) = \frac{1}{\pi} \int_0^\pi d\theta \int_0^\infty d\rho_0 p_e(\rho_0;M) \sum_{n=0}^\infty \frac{\left(-\frac{\rho_0}{\gamma_0}\right)^n}{n!} \sum_{m=0}^\infty \frac{\left(2\sqrt{\delta_0} \cos\theta \sqrt{\frac{\rho_0}{\gamma_0}}\right)^m}{m!}$$

$$= \frac{1}{\pi} \int_0^\pi d\theta \int_0^\infty d\rho_0 p_e(\rho_0;M) \sum_{n=0}^\infty \left(\frac{\rho_0}{\gamma_0}\right)^n \frac{(-1)^n}{n!} \sum_{m=0}^\infty \left(\frac{\rho_0}{\gamma_0}\right)^{\frac{m}{2}} \frac{\left(2\sqrt{\delta_0} \cos\theta\right)^m}{m!}$$

$$= \frac{1}{\pi} \int_0^\pi d\theta \int_0^\infty d\rho_0 p_e(\rho_0;M) \sum_{n=0}^\infty \sum_{m=0}^\infty \left(\frac{\rho_0}{\gamma_0}\right)^{n+\frac{m}{2}} \frac{(-1)^n}{n!} \frac{\left(2\sqrt{\delta_0} \cos\theta\right)^m}{m!}$$

define $\alpha = n + \frac{m}{2}$

$$= \int_0^\infty d\rho_0 p_e(\rho_0;M) + \frac{1}{\pi} \int_0^\pi d\theta \int_0^\infty d\rho_0 p_e(\rho_0;M) \sum_{\substack{n=0 \\ n \neq m \neq 0}}^\infty \sum_{m=0}^\infty \left(\frac{\rho_0}{\gamma_0}\right)^\alpha \frac{(-1)^n}{n!} \frac{\left(2\sqrt{\delta_0} \cos\theta\right)^m}{m!}$$

$$= \int_0^\infty d\rho_0 p_e(\rho_0;M) + \frac{1}{\pi} \int_0^\pi d\theta \sum_{\substack{n=0 \\ n \neq m \neq 0}}^\infty \sum_{m=0}^\infty \frac{(-1)^n}{n!} \frac{\left(2\sqrt{\delta_0} \cos\theta\right)^m}{m!} \frac{1}{\gamma_0^\alpha} \int_0^\infty \rho_0^\alpha p_e(\rho_0;M) d\rho_0$$

$$= \lambda_{1,M} + \frac{1}{\pi} \int_0^\pi d\theta \sum_{\substack{n=0 \\ n \neq m \neq 0}}^\infty \sum_{m=0}^\infty \frac{(-1)^n}{n!} \frac{\left(2\sqrt{\delta_0} \cos\theta\right)^m}{m!} q_{nm0}$$

where $\lambda_{1,M} = \int_0^\infty d\rho_0 p_e(\rho_0;M)$ and $q_{nm0} = \frac{1}{\gamma_0^\alpha} \int_0^\infty \rho_0^\alpha p_e(\rho_0;M) d\rho_0$.

31

If the integral in $q_{nm0}$ has a singularity of order less than $\alpha$, then

$$\gamma_0 e^{\delta_0} P_e(1;M) \leq \lambda_{1,M} + \frac{1}{\pi} \int_0^\pi d\theta \sum_{\substack{n=0 \\ n \neq m \neq 0}}^\infty \sum_{m=0}^\infty \frac{(-1)^n}{n!} \frac{\left(2\sqrt{\delta_0} \cos\theta\right)^m}{m!} \frac{\alpha}{\gamma_0^\alpha}. \qquad (3.13)$$

By taking the limit of (3.13) as $\gamma_0 \to \infty$, the second term in (.) become zero.

$$\lambda_{1,M} = \lim_{\gamma_0 \to \infty} \left[\gamma_0 e^{\delta_0} P_e(1;M)\right] = \int_0^\infty d\rho_0 p_e(\rho_0;M)$$

For any $K$,

$$P_e(K;M) = \frac{e^{-\Delta_K}}{\Gamma_K} \int_0^\infty d\rho_0 ... \int_0^\infty d\rho_{K-1} \prod_{k=0}^{K-1} e^{-\frac{\rho_k}{r_k}} I_0\left(2\sqrt{\frac{\delta_k \rho_k}{\gamma_k}}\right) p_e(\rho_0,...,\rho_{K-1};M),$$

so we have

$$\Gamma_K e^{\Delta_K} P_e(K;M) = \int_0^\infty d\rho_1 ... \int_0^\infty d\rho_{K-1} \prod_{k=1}^{K-1} e^{-\frac{\rho_k}{r_k}} I_0\left(2\sqrt{\frac{\delta_k \rho_k}{\gamma_k}}\right)$$

$$\cdot \int_0^\infty d\rho_0 e^{-\frac{\rho_0}{r_0}} I_0\left(2\sqrt{\frac{\delta_0 \rho_0}{\gamma_0}}\right) p_e(\rho_0,...,\rho_{K-1};M).$$

Again, by using the trigonometric form of $I_0(.)$, we have

$$\Gamma_K e^{\Delta_K} P_e(K;M) = \int_0^\infty d\rho_1 ... \int_0^\infty d\rho_{K-1} \prod_{k=1}^{K-1} e^{-\frac{\rho_k}{\gamma_k}} I_0\left(2\sqrt{\frac{\delta_k \rho_k}{\gamma_k}}\right)$$

$$\cdot \int_0^\infty d\rho_0 e^{-\frac{\rho_0}{\gamma_0}} \frac{1}{\pi} \int_0^\pi d\theta e^{2\sqrt{\frac{\delta_0 \rho_0}{\gamma_0}} \cos\theta} p_e(\rho_0,...,\rho_{K-1};M).$$

Similar to the derivation for the case of $K=1$, we expand the two exponents using Taylor series expansion and obtain

$$\Gamma_K e^{\Delta_K} P_e(K,M) = \int_0^\infty d\rho_1 ... \int_0^\infty d\rho_{K-1} \prod_{k=1}^{K-1} e^{-\frac{\rho_k}{\gamma_k}} I_0\left(2\sqrt{\frac{\delta_k \rho_k}{\gamma_k}}\right)$$

$$\cdot \frac{1}{\pi} \int_0^\pi d\theta \int_0^\infty d\rho_0 \sum_{n_0=0}^\infty \frac{\left(-\frac{\rho_0}{\gamma_0}\right)^{n_0}}{n_0!} \sum_{m_0=0}^\infty \frac{\left(2\sqrt{\delta_0} \cos\theta \sqrt{\frac{\rho_0}{\gamma_0}}\right)^{m_0}}{m_0!} p_e(\rho_0,...,\rho_{K-1};M)$$

32

$$= \int_0^\infty d\rho_1 \ldots \int_0^\infty d\rho_{K-1} \prod_{k=1}^{K-1} e^{-\frac{\rho_k}{\gamma_k}} I_0\left(2\sqrt{\frac{\delta_k \rho_k}{\gamma_k}}\right) \int_0^\infty d\rho_0 p_e(\rho_0, \ldots, \rho_{K-1}; M)$$

$$+ \int_0^\infty d\rho_1 \ldots \int_0^\infty d\rho_{K-1} \prod_{k=1}^{K-1} e^{-\frac{\rho_k}{\gamma_k}} I_0\left(2\sqrt{\frac{\delta_k \rho_k}{\gamma_k}}\right)$$

$$\cdot \frac{1}{\pi} \int_0^\pi d\theta \int_0^\infty d\rho_0 p_e(\rho_0 \ldots \rho_{K-1}; M) \sum_{\substack{n_0=0 \\ n_0 \neq m_0 \neq 0}}^\infty \sum_{m_0=0}^\infty \left(\frac{\rho_0}{\gamma_0}\right)^\alpha \frac{(-1)^{n_0}}{n_0!} \frac{\left(2\sqrt{\delta_0} \cos\theta\right)^{m_0}}{m_0!}$$

$$= \int_0^\infty d\rho_0 \int_0^\infty d\rho_1 \ldots \int_0^\infty d\rho_{K-1} \prod_{k=1}^{K-1} e^{-\frac{\rho_k}{\gamma_k}} I_0\left(2\sqrt{\frac{\delta_k \rho_k}{\gamma_k}}\right) p_e(\rho_0, \ldots, \rho_{K-1}; M)$$

$$+ \int_0^\infty d\rho_1 \ldots \int_0^\infty d\rho_{K-1} \prod_{k=1}^{K-1} e^{-\frac{\rho_k}{\gamma_k}} I_0\left(2\sqrt{\frac{\delta_k \rho_k}{\gamma_k}}\right)$$

$$\cdot \frac{1}{\pi} \int_0^\pi d\theta \sum_{\substack{n_0=0 \\ n_0 \neq m_0 \neq 0}}^\infty \sum_{m_0=0}^\infty \frac{(-1)^{n_0}}{n_0!} \frac{\left(2\sqrt{\delta_0} \cos\theta\right)^{m_0}}{m_0!} \frac{1}{\gamma_0^\alpha} \int_0^\infty \rho_0^\alpha p_e(\rho_0, \ldots, \rho_{K-1}; M) d\rho_0$$

$$= \int_0^\infty d\rho_0 \int_0^\infty .d\rho_1 \ldots \int_0^\infty d\rho_{K-1} \prod_{k=1}^{K-1} e^{-\frac{\rho_k}{\gamma_k}} I_0\left(2\sqrt{\frac{\delta_k \rho_k}{\gamma_k}}\right) p_e(\rho_0, \ldots, \rho_{K-1}; M)$$

$$+ \int_0^\infty d\rho_1 \ldots \int_0^\infty d\rho_{K-1} \prod_{k=1}^{K-1} e^{-\frac{\rho_k}{\gamma_k}} I_0\left(2\sqrt{\frac{\delta_k \rho_k}{\gamma_k}}\right) \cdot \frac{1}{\pi} \int_0^\pi d\theta \sum_{\substack{n_0=0 \\ n_0 \neq m_0 \neq 0}}^\infty \sum_{m_0=0}^\infty \frac{(-1)^{n_0}}{n_0!} \frac{\left(2\sqrt{\delta_0} \cos\theta\right)^{m_0}}{m_0!} q_{nm0}$$

where $\quad q_{nm0} = \dfrac{1}{\gamma_0^\alpha} \displaystyle\int_0^\infty \rho_0^\alpha p_e(\rho_0 \ldots \rho_{K-1}; M) d\rho_0$ .

If the integral in $q_{nm0}$ has a singularity of order less than $\alpha$ , then

$$\Gamma_K e^{\Delta_K} P_e(K; M) = \int_0^\infty d\rho_0 \int_0^\infty .d\rho_1 \ldots \int_0^\infty d\rho_{K-1} \prod_{k=1}^{K-1} e^{-\frac{\rho_k}{\gamma_k}} I_0\left(2\sqrt{\frac{\delta_k \rho_k}{\gamma_k}}\right) p_e(\rho_0, \ldots, \rho_{K-1}; M)$$

$$+ \int_0^\infty d\rho_1 \ldots \int_0^\infty d\rho_{K-1} \prod_{k=1}^{K-1} e^{-\frac{\rho_k}{\gamma_k}} I_0\left(2\sqrt{\frac{\delta_k \rho_k}{\gamma_k}}\right) \cdot \frac{1}{\pi} \int_0^\pi d\theta \sum_{\substack{n_0=0 \\ n_0 \neq m_0 \neq 0}}^\infty \sum_{m_0=0}^\infty \frac{(-1)^{n_0}}{n_0!} \frac{\left(2\sqrt{\delta_0} \cos\theta\right)^{m_0}}{m_0!} \frac{\alpha}{\gamma_0^\alpha} \quad (3.14)$$

33

By taking the limit of (3.14) as $\gamma_0 \to \infty$, the second term become zero and therefore

we have

$$\Gamma_K e^{\Delta_K} P_e(K;M) = \int_0^\infty d\rho_0 \int_0^\infty d\rho_1 ... \int_0^\infty d\rho_{K-1} \prod_{k=1}^{K-1} e^{-\frac{\rho_k}{\gamma_k}} I_0\left(2\sqrt{\frac{\delta_k \rho_k}{\gamma_k}}\right) p_e(\rho_0,...,\rho_{K-1};M)$$

We perform the above steps $K-1$ times, then we obtain

$$\lambda_{K,M} = \lim_{\gamma_0,...,\gamma_{K-1} \to \infty}\left[\Gamma_K e^{\Delta_K} P_e(K;M)\right] = \int_0^\infty ... \int_0^\infty p_e(\rho_0,...,\rho_{K-1};M)d\rho_0...d\rho_{K-1} \quad \blacksquare$$

## 3.3 Two Theorems for Special Cases

Theorem 2[1]: If $p_e(\boldsymbol{\rho};M) = p_e(\rho;M)$ with $\rho = \sum_{k=0}^{K-1} \rho_k$ i.e., $p_e(\boldsymbol{\rho};M)$ is a

function of the sum of the received SNRs in multiple paths as in MRC, then $\lambda_{K,M}$ is

given by

$$\lambda_{K,M} = \frac{1}{(K-1)!}\int_0^\infty p_e(\rho;M)\rho^{K-1}d\rho \tag{3.15}$$

Proof:

According to Theorem1, we have

$$\lambda_{K,M} = \int_0^\infty ... \int_0^\infty p_e(\rho_0,...,\rho_{K-1};M)d\rho_0...d\rho_{K-1}$$

Since $p_e(\boldsymbol{\rho};M) = p_e(\rho;M)$, we have

$$p_e(\rho_0,...,\rho_{K-1};M) = p_e(\rho;M)$$

Therefore,

$$\lambda_{K,M} = \int_0^\infty ... \int_0^\infty p_e(\rho;M)d\rho_0...d\rho_{K-1}$$

We introduce the new variables:

$$\begin{cases} \rho = \rho_0 + \rho_1 + ... + \rho_{K-1} \\ \quad x_1 = \rho_1 \\ \quad ... \\ \quad x_{K-1} = \rho_{K-1} \end{cases}$$

34

So we have

$$\begin{cases} \rho_0 = \rho - x_1 - ... - x_{K-1} > 0 \\ \quad \rho_1 = x_1 > 0 \\ \quad ... \\ \quad \rho_{K-1} = x_{K-1} > 0 \end{cases}$$

and $\rho_0, ..., \rho_{K-1}$ are independent

The Jacobian of the transformation is:

$$J = \begin{vmatrix} \dfrac{\partial \rho_0}{\partial \rho} & \dfrac{\partial \rho_1}{\partial \rho} & ... & \dfrac{\partial \rho_{K-1}}{\partial \rho} \\ \dfrac{\partial \rho_0}{\partial x_1} & \dfrac{\partial \rho_1}{\partial x_1} & ... & \dfrac{\partial \rho_{K-1}}{\partial x_1} \\ ... & ... & ... & ... \\ \dfrac{\partial \rho_0}{\partial x_{K-1}} & \dfrac{\partial \rho_1}{\partial x_{K-1}} & ... & \dfrac{\partial \rho_{K-1}}{\partial x_{K-1}} \end{vmatrix} = \begin{vmatrix} 1 & 0 & ... & 0 \\ -1 & 1 & 0 & ... \\ ... & ... & ... & ... \\ -1 & 0 & ... & 1 \end{vmatrix} = 1$$

Therefore

$$\lambda_{K,M} = \int_0^\infty ... \int_0^\infty p_e(\rho;M)|J| d\rho dx_1 ... dx_{K-1}$$

$$= \int_0^\infty d\rho p_e(\rho;M) V_{K-1}(\rho) \tag{3.16}$$

where

$$V_{K-1}(\rho) = \int_0^\rho dx_1 \int_0^{\rho-x_1} dx_2 ... \int_0^{\rho-\sum_{k=1}^{K-2} x_k} dx_{K-1}$$

$$= \int_0^\rho dx_1 \int_0^{\rho-x_1} dx_2 ... \int_0^{\rho-\sum_{k=1}^{K-3} x_k} \left( \rho - \sum_{k=1}^{K-2} x_k \right) dx_{K-2}$$

$$= \int_0^\rho dx_1 \int_0^{\rho-x_1} dx_2 ... \int_0^{\rho-\sum_{k=1}^{K-3} x_k} \left( \rho - \sum_{k=1}^{K-3} x_k - x_{K-2} \right) dx_{K-2}$$

Assuming $y_{K-2} = \rho - \sum_{k=1}^{K-3} x_k - x_{K-2}$, we obtain:

$$V_{K-1}(\rho) = \int_0^\rho dx_1 \int_0^{\rho-x_1} dx_2 ... \int_{\rho-\sum_{k=1}^{K-3} x_k}^0 y_{K-2} d(-y_{K-2})$$

35

$$= \int_0^\rho dx_1 \int_0^{\rho-x_1} dx_2 ... (-y_{K-2}^2 / 2) \Big|_{\rho-\sum_{k=1}^{K-3} x_k}^{0}$$

$$= \int_0^\rho dx_1 \int_0^{\rho-x_1} dx_2 ... \int_0^{\rho-\sum_{k=1}^{K-4} x_k} \left( \rho - \sum_{k=1}^{K-3} x_k \right)^2 / 2 dx_{K-3}$$

$$= \int_0^\rho dx_1 \int_0^{\rho-x_1} dx_2 ... \int_0^{\rho-\sum_{k=1}^{K-4} x_k} \left( \rho - \sum_{k=1}^{K-4} x_k - x_{K-3} \right)^2 / 2 dx_{K-3}$$

Assuming $y_{K-3} = \rho - \sum_{k=1}^{K-4} x_k - x_{K-3}$ , we obtain:

$$V_{K-1}(\rho) = \int_0^\rho dx_1 \int_0^{\rho-x_1} dx_2 ... \int_{\rho-\sum_{k=1}^{K-4} x_k}^{0} y_{K-3}^2 / 2 d(-y_{K-3})$$

$$= \int_0^\rho dx_1 \int_0^{\rho-x_1} dx_2 ... \left(- y_{K-3}^3 / 6\right) \Big|_{\rho-\sum_{k=1}^{K-4} x_k}^{0}$$

$$= \int_0^\rho dx_1 \int_0^{\rho-x_1} dx_2 ... \int_0^{\rho-\sum_{k=1}^{K-5} x_k} \left( \rho - \sum_{k=1}^{K-4} x_k \right)^3 / 3! dx_{K-4}$$

$$= ...$$

$$= \int_0^\rho dx_1 \int_0^{\rho-x_1} (\rho - x_1 - x_2)^{K-3} / (K-3)! dx_2$$

$$...$$

$$= \int_0^\rho dx_1 (\rho - x_1)^{K-2} / (K-2)!$$

$$= \rho^{K-1} / (K-1)!.$$

Therefore, (3.15) can be transformed as

$$\lambda_{K,M} = 1/(K-1)! \int_0^\infty \rho^{K-1} p_e(\rho;M) d\rho \qquad\qquad \blacksquare$$

Theorem 3[1]: If $p_e(\rho;M) = p_e(\rho_t;M)$ with $\rho_t = \left[ \sum_{k=0}^{K-1} \sqrt{\rho_k} \right]^2$ , i.e., $p_e(\rho;M)$

is a function of the received amplitudes in multipaths as in EGC, then $\lambda_{K,M}$ is given

by

$$\lambda_{K,M} = \frac{2^{K-1}}{(2K-1)!} \int_0^\infty p_e(\rho_t;M)\rho_t^{K-1}d\rho_t.$$ (3.17)

Proof:

According to Theorem 1, we have

$$\lambda_{K,M} = \int_0^\infty ... \int_0^\infty p_e(\rho_0,...,\rho_{K-1};M)d\rho_0...d\rho_{K-1}.$$

Assuming $\rho_K = A_K^2$, we obtain

$$\lambda_{K,M} = \int_0^\infty ... \int_0^\infty p_e(A_0^2,...,A_{K-1}^2;M)dA_0^2...dA_{K-1}^2$$

Since $p_e(\boldsymbol{\rho};M) = p_e(\rho_t;M)$,

$$p_e(\rho_0,...,\rho_{K-1};M) = p_e(\boldsymbol{\rho};M) = p_e(\rho_t;M).$$

Therefore, $\lambda_{K,M} = \int_0^\infty ... \int_0^\infty 2^K p_e(A_t^2;M)A_0...A_{K-1}dA_0...dA_{K-1}.$

We introduce the new variables

$$\begin{cases} A_t = A_0 + A_1 + ... + A_{K-1} \\ \quad x_1 = A_1 \\ \quad ... \\ \quad x_{K-1} = A_{K-1} \end{cases}.$$

So we have

$$\begin{cases} A_0 = A_t - x_1 - ... - x_{K-1} > 0 \\ \quad A_1 = x_1 > 0 \\ \quad ... \\ \quad A_{K-1} = x_{K-1} > 0 \end{cases}.$$

The Jacobian of the transformation is:

$$J = \begin{vmatrix} \dfrac{\partial A_0}{\partial A_t} & \dfrac{\partial A_1}{\partial A_t} & ... & \dfrac{\partial A_{K-1}}{\partial A_t} \\ \dfrac{\partial A_0}{\partial x_1} & \dfrac{\partial A_1}{\partial x_1} & ... & \dfrac{\partial A_{K-1}}{\partial x_1} \\ \dfrac{...}{\partial A_0} & \dfrac{...}{\partial A_1} & ... & \dfrac{...}{\partial A_{K-1}} \\ \dfrac{\partial A_0}{\partial x_{K-1}} & \dfrac{\partial A_1}{\partial x_{K-1}} & ... & \dfrac{\partial A_{K-1}}{\partial x_{K-1}} \end{vmatrix} = \begin{vmatrix} 1 & 0 & ... & 0 \\ -1 & 1 & 0 & ... \\ ... & ... & ... & ... \\ -1 & 0 & ... & 1 \end{vmatrix} = 1.$$

We obtain: $\lambda_{K,M} = \int_0^\infty ... \int_0^\infty 2^K p_e(A_t^2;M)A_t x_1...x_{K-1}|J|dA_t dx_1...dx_{K-1}$

37

$$= \int_0^\infty dA_t \, p_e(A_t^2; M) U_{K-1}(A_t) \tag{3.18}$$

where $U_{K-1}(A_t) = 2^K \int_0^{A_t} x_1 dx_1 \int_0^{A_t - x_1} x_2 dx_2 \dots \int_0^{A_t - \sum_{k=1}^{K-2} x_k} x_{K-1} \left( A_t - \sum_{k=1}^{K-1} x_k \right) dx_{K-1}$

$$= 2^K \int_0^{A_t} x_1 dx_1 \int_0^{A_t - x_1} x_2 dx_2 \dots \int_0^{\rho - \sum_{k=1}^{K-2} x_k} \left( A_t - \sum_{k=1}^{K-2} x_k - x_{K-1} \right) x_{K-1} dx_{K-1} \ .$$

Assuming $y_{K-1} = A_t - \sum_{k=1}^{K-2} x_k - x_{K-1}$ , we obtain

$$U_{K-1}(A_t) = 2^K \int_0^{A_t} x_1 dx_1 \int_0^{A_t - x_1} x_2 dx_2 \dots \int_{\rho - \sum_{k=1}^{K-2} x_k}^{0} y_{K-1} \left( A_t - \sum_{k=1}^{K-2} x_k - y_{K-1} \right) d(-y_{K-1})$$

$$= 2^K \int_0^{A_t} x_1 dx_1 \int_0^{A_t - x_1} x_2 dx_2 \dots \left[ y_{K-1}^3 / 3 - y_{K-1}^2 \left( A_t - \sum_{k=1}^{K-2} x_k \right) / 2 \right] \Bigg|_{\rho - \sum_{k=1}^{K-2} x_k}^{0}$$

$$= 2^K \int_0^{A_t} x_1 dx_1 \int_0^{A_t - x_1} x_2 dx_2 \dots \int_0^{A_t - \sum_{k=1}^{K-3} x_k} x_{K-2} \left( A_t - \sum_{k=1}^{K-2} x_k \right)^3 / 6 \, dx_{K-2}$$

$$= 2^K \int_0^{A_t} x_1 dx_1 \int_0^{A_t - x_1} x_2 dx_2 \dots \int_0^{A_t - \sum_{k=1}^{K-3} x_k} x_{K-2} \left( A_t - \sum_{k=1}^{K-3} x_k - x_{K-2} \right)^3 / 3! \, dx_{K-2} \ .$$

Assuming $y_{K-2} = A_t - \sum_{k=1}^{K-3} x_k - x_{K-2}$ , we obtain

$$U_{K-1}(A_t) = 2^K \int_0^{A_t} x_1 dx_1 \int_0^{A_t - x_1} x_2 dx_2 \dots \int_{\rho - \sum_{k=1}^{K-3} x_k}^{0} y_{K-2}^3 \left( A_t - \sum_{k=1}^{K-3} x_k - y_{K-2} \right) / 6 \, d(-y_{K-2})$$

$$= 2^K \int_0^{A_t} x_1 dx_1 \int_0^{A_t - x_1} x_2 dx_2 \dots \left[ y_{K-2}^5 / 30 - y_{K-2}^4 \left( A_t - \sum_{k=1}^{K-3} x_k \right) / 24 \right] \Bigg|_{\rho - \sum_{k=1}^{K-3} x_k}^{0}$$

$$= 2^K \int_0^{A_t} x_1 dx_1 \int_0^{A_t - x_1} x_2 dx_2 \dots \int_0^{A_t - \sum_{k=1}^{K-4} x_k} x_{K-3} \left( A_t - \sum_{k=1}^{K-3} x_k \right)^5 / 5! \, dx_{K-3}$$

$\dots$

$$= 2^K \int_0^{A_t} x_1 dx_1 \int_0^{A_t - x_1} x_2 dx_2 (A_t - x_1 - x_2)^{2K-5} / (2K - 5)!$$

$$= 2^K \int_0^{A_t} x_1 dx_1 (A_t - x_1)^{2K-3} / (2K - 3)!$$

38

$$= 2^K A_t^{2K-1} / (2K-1)!.$$

Therefore, (3.18) can be transformed as

$$\lambda_{K,M} = \int_0^\infty dA_t p_e(A_t^2; M) 2^K A_t^{2K-1} / (2K-1)!$$

$$= 2^{K-1} / (2K-1)! \int_0^\infty dA_t^2 p_e(A_t^2; M) A_t^{2K-2}$$

$$= 2^{K-1} / (2K-1)! \int_0^\infty d\rho_t p_e(\rho_t; M) \rho_t^{K-1} \qquad \blacksquare$$

## 3.4 Asymptotic Performance of M-ary Signaling

Before the discussion of asymptotic performance of M-ary signaling, two lemmas

which will be used in the following discussion, will be proved first.

$$\text{Lemma 1:} \quad \frac{1}{(K-1)!} \int_0^\infty \rho^{K-1} \exp(-\rho C) d\rho = \frac{1}{C^K}$$

Proof: $\dfrac{1}{(K-1)!} \int_0^\infty d\rho \rho^{K-1} \exp(-\rho C)$

$$= \frac{1}{(-C)(K-1)!} \int_0^\infty \rho^{K-1} d\exp(-\rho C)$$

$$= \frac{1}{(-C)(K-1)!} \left[ \rho^{K-1} \exp(-\rho C) \Big|_0^\infty - \int_0^\infty \exp(-\rho C) d\rho^{K-1} \right]$$

$$= \frac{1}{C(K-1)!} \int_0^\infty \exp(-\rho C) d\rho^{K-1}$$

$$= \frac{1}{-C^2(K-2)!} \int_0^\infty \rho^{K-2} d\exp(-\rho C)$$

$$= \frac{1}{C(K-2)!} \int_0^\infty \rho^{K-2} \exp(-\rho C) d\rho$$

$$\ldots$$

$$= \frac{1}{C^K} \qquad \blacksquare$$

39

Lemma 2: $\int_{\theta_1}^{\theta_2} \sin^{2K}\theta d\theta = 2^{-2K}\left[\dfrac{(2K)!}{K!K!}(\theta_2-\theta_1)+2\sum_{l=1}^{K}\binom{2K}{K-l}\dfrac{(\sin 2\theta_2 l-\sin 2\theta_1 l)}{2l}\right]$

Proof: Using Euler's expression $\sin^{2K}\theta = 2^{-2K}\left[\binom{2K}{K}+2\sum_{l=1}^{K}\binom{2K}{K-l}(-1)^{l}\cos 2\theta l\right]$,

we obtain

$$\int_{\theta_1}^{\theta_2} \sin^{2K}\theta d\theta = 2^{-2K}\int_{\theta_1}^{\theta_2}\left[\binom{2K}{K}+2\sum_{l=1}^{K}\binom{2K}{K-l}(-1)^{l}\cos 2\theta l\right]d\theta$$

$$= 2^{-2K}\left[\dfrac{(2K)!}{K!K!}(\theta_2-\theta_1)+2\sum_{l=1}^{K}\binom{2K}{K-l}\dfrac{(\sin 2\theta_2 l-\sin 2\theta_1 l)}{2l}\right]\qquad\blacksquare$$

It has been shown that the SNR of the decision variable $\xi$ is equal to $\rho$ for

coherent MRC, and is equal to $\rho_t/K$ for coherent EGC [8], where as

discussed in hapter 2.

$$\rho = \sum_{k=0}^{K-1}\rho_k \qquad\qquad (3.19)$$

$$\rho_t = [\sum_{k=0}^{K-1}A_k]^2 \qquad\qquad (3.20)$$

**MPSK signaling**

The asymptotic performance of MRC-MPSK is given as[1]

$$\lambda_{b_K,M} = \dfrac{2^{-2K}}{[\log_2 M \sin^2(\pi/M)]^K}\left[\binom{2K}{K}\left(\dfrac{M-1}{M}\right)-\sum_{l=1}^{K}\binom{2K}{K-l}(-1)^{l}\dfrac{\sin(2\pi l/M)}{\pi l}\right](3.20)$$

Proof:

Based on the definition of $\lambda_{b_K,M}$ in (3.11) and the result of (3.15) in Theorem 2, we

have

40

$$\lambda_{b_K,M} = \frac{\lambda_{K,M}}{(\log_2 M)^K}$$

$$= \frac{1}{(\log_2 M)^K (K-1)!} \int_0^\infty d\rho\, p_e(\rho,M)\rho^{K-1}$$

Based on the expression of $p_e(\xi;M)$ for MPSK signaling in (2.7), we have:

$$\lambda_{b_K,M} = \frac{1}{(\log_2 M)^K (K-1)!} \int_0^\infty d\rho\, \rho^{K-1} \frac{1}{\pi} \int_{\pi/M}^{\pi} d\theta \exp\left[-\rho\frac{\sin^2(\pi/M)}{\sin^2\theta}\right]$$

$$= \frac{1}{(\log_2 M)^K \pi} \int_{\pi/M}^{\pi} d\theta \frac{1}{(K-1)!} \int_0^\infty d\rho\, \rho^{K-1} \exp\left[-\rho\frac{\sin^2(\pi/M)}{\sin^2\theta}\right]$$

Using Lemma 1, we have

$$\frac{1}{(K-1)!} \int_0^\infty d\rho\, \rho^{K-1} \exp\left[-\rho\frac{\sin^2(\pi/M)}{\sin^2\theta}\right] = \frac{\sin^{2K}\theta}{\sin^{2K}(\pi/M)},$$

and therefore

$$\lambda_{b_K,M} = \frac{1}{(\log_2 M)^K \pi} \int_{\pi/M}^{\pi} d\theta \frac{\sin^{2K}\theta}{\sin^{2K}(\pi/M)}.$$

Using Lemma 2 with $\theta_1 = \pi/M$, $\theta_2 = \pi$, we obtain:

$$\lambda_{b_K,M} = \frac{2^{-2K}}{(\log_2 M)^K \pi \sin^{2K}(\pi/M)} \int_{\pi/M}^{\pi} d\theta \left[\binom{2K}{K} + 2\sum_{l=1}^{K}\binom{2K}{K-l}(-1)^l \cos(2\theta l)\right]$$

$$= \frac{2^{-2K}}{[\log_2 M \sin^2(\pi/M)]^K} \left[\binom{2K}{K}\left(\frac{M-1}{M}\right) - \sum_{l=1}^{K}\binom{2K}{K-l}(-1)^l \frac{\sin(2\pi l/M)}{\pi l}\right] \quad \blacksquare$$

The asymptotic performance of EGC-MPSK is given as [1]

$$\lambda_{b_K,M} = \frac{2^{-K} K! K^K}{[(\log_2 M)\sin^2(\pi/M)]^K (2K)!} \left[\binom{2K}{K}\left(\frac{M-1}{M}\right) - \sum_{l=1}^{K}\binom{2K}{K-l}(-1)^l \frac{\sin(2\pi l/M)}{\pi l}\right]$$

$$(3.21).$$

Proof:

Based on the definition of $\lambda_{b_K,M}$ in (3.11) and the result of (3.17) in Theorem 3, we

have

41

$$\lambda_{b_K,M} = \frac{\lambda_{K,M}}{(\log_2 M)^K}$$

$$= \frac{2^{K-1}}{(\log_2 M)^K (2K-1)!} \int_0^\infty p_e(\rho_t; M)\rho_t^{K-1} d\rho_t$$

Based on the expression of $p_e(\xi; M)$ for MPSK signaling in (2.7) and (3.19), we

obtain:

$$\lambda_{b_K,M} = \frac{2^{K-1}}{(\log_2 M)^K (2K-1)!} \int_0^\infty d\rho_t \rho_t^{K-1} \frac{1}{\pi} \int_{\pi/M}^\pi d\theta \exp\left[-\rho_t \frac{\sin^2(\pi/M)}{K \sin^2 \theta}\right]$$

$$= \frac{2^{K-1}(K-1)!}{(\log_2 M)^K \pi (2K-1)!} \int_{\pi/M}^\pi d\theta \frac{1}{(K-1)!} \int_0^\infty d\rho_t \rho_t^{K-1} \exp\left[-\rho_t \frac{\sin^2(\pi/M)}{K \sin^2 \theta}\right]$$

Using Lemma 1, we have

$$\frac{1}{(K-1)!} \int_0^\infty d\rho_t \rho_t^{K-1} \exp\left[-\rho_t \frac{\sin^2(\pi/M)}{K \sin^2 \theta}\right] = \frac{K^K \sin^{2K} \theta}{\sin^{2K}(\pi/M)}$$

and therefore

$$\lambda_{b_K,M} = \frac{2^{K-1}(K-1)!}{(\log_2 M)^K \pi (2K-1)!} \int_{\pi/M}^\pi \frac{K^K \sin^{2K} \theta}{\sin^{2K}(\pi/M)} d\theta$$

Using Lemma 2 with $\theta_1 = \pi/M$, $\theta_2 = \pi$, we obtain:

$$\lambda_{b_K,M} = \frac{2^{-2K}2^{K-1}(K-1)!K^K}{(\log_2 M)^K \pi \sin^{2K}(\pi/M)(2K-1)!} \int_{\pi/M}^\pi \left[\binom{2K}{K} + 2\sum_{l=1}^K \binom{2K}{K-l}(-1)^l \cos(2\theta l)\right] d\theta$$

$$= \frac{2^{-K}K!K^K}{[(\log_2 M)\sin^2(\pi/M)]^K (2K)!} \left[\binom{2K}{K}\left(\frac{M-1}{M}\right) - \sum_{l=1}^K \binom{2K}{K-l}(-1)^l \frac{\sin(2\pi l/M)}{\pi l}\right] \blacksquare$$

**MPAM signaling**

The asymptotic error rate performance of MRC-MPAM is given [1]

$$\lambda_{b_K,M} = \frac{M-1}{M} \left[\frac{M^2-1}{12\log_2 M}\right]^K \binom{2K}{K} \tag{3.22}$$

42

Proof:

Since the conditional SER of MPAM signaling is $p_e(\xi;M) = \dfrac{M-1}{M} erfc\left(\sqrt{\dfrac{3\xi}{(M^2-1)}}\right)$

as given in (2.9), according to Theorem 2, we have

$$\lambda_{b_K,M} = \frac{1}{(K-1)!(\log_2 M)^K} \int_0^\infty d\rho \rho^{K-1} \frac{M-1}{M} erfc\left(\sqrt{\frac{3\rho}{M^2-1}}\right).$$

From $erfc(y) = \dfrac{1}{\pi}\int_0^\pi d\theta \exp\left(\dfrac{-y^2}{\sin^2\theta}\right)$, we have

$$\lambda_{b_K,M} = \frac{1}{(K-1)!(\log_2 M)^K} \int_0^\infty d\rho \rho^{K-1} \frac{M-1}{M} \frac{1}{\pi} \int_0^\pi d\theta \exp\left[\frac{-3\rho}{(M^2-1)\sin^2\theta}\right]$$

$$= \frac{M-1}{(\log_2 M)^K \pi M} \int_0^\pi d\theta \frac{1}{(K-1)!} \int_0^\infty d\rho \rho^{K-1} \exp\left[-\rho\frac{3}{(M^2-1)\sin^2\theta}\right].$$

Using Lemma 1, we obtain

$$\lambda_{b_K,M} = \frac{M-1}{(\log_2 M)^K \pi M} \int_0^\pi d\theta \frac{\sin^{2K}\theta(M^2-1)^K}{3^K}$$

$$= \frac{M-1}{M}\left[\frac{M^2-1}{3\log_2 M}\right]^K \frac{1}{\pi}\int_0^\pi d\theta \sin^{2K}\theta.$$

Using Lemma 2, we obtain:

$$\lambda_{b_K,M} = \frac{M-1}{M}\left[\frac{M^2-1}{3(\log_2 M)}\right]^K \frac{2^{-2K}\pi}{\pi}\frac{(2K)!}{K!K!}$$

$$= \frac{M-1}{M}\left[\frac{M^2-1}{12\log_2 M}\right]^K \binom{2K}{K}. \qquad\blacksquare$$

The asymptotic performance of EGC-MPAM is given as [1]

$$\lambda_{b_K,M} = \frac{M-1}{M}\left[\frac{M^2-1}{6(\log_2 M)}\right]^K \frac{K^K}{K!}. \qquad (3.23)$$

Proof:

Since the conditional SER of MPAM signaling is $p_e(\xi;M) = \dfrac{M-1}{M} erfc\left(\sqrt{\dfrac{3\xi}{(M^2-1)}}\right)$

43

as given in (2.9) and (3.19), according to Theorem 3, we have

$$\lambda_{b_K,M} = \frac{2^{K-1}}{(2K-1)!(\log_2 M)^K} \int_0^\infty d\rho_t \rho_t^{K-1} \frac{M-1}{M} erfc\left(\sqrt{\frac{3\rho_t}{K(M^2-1)}}\right).$$

From $erfc(y) = \frac{1}{\pi}\int_0^\pi d\theta \exp\left[\frac{-y^2}{\sin^2\theta}\right]$ , we have

$$\lambda_{b_K,M} = \frac{2^{K-1}}{(2K-1)!(\log_2 M)^K} \int_0^\infty d\rho_t \rho_t^{K-1} \frac{M-1}{M}\frac{1}{\pi}\int_0^\pi d\theta \exp\left[\frac{-3\rho_t}{K(M^2-1)\sin^2\theta}\right]$$

$$= \frac{2^{K-1}(M-1)(K-1)!}{(\log_2 M)^K \pi M(2K-1)!} \int_0^\pi d\theta \frac{1}{(K-1)!}\int_0^\infty d\rho_t \rho_t^{K-1} \exp\left[-\rho_t \frac{3}{K(M^2-1)\sin^2\theta}\right]$$

Using Lemma 1, we obtain

$$\lambda_{b_K,M} = \frac{2^{K-1}(M-1)(K-1)!}{(\log_2 M)^K \pi M(2K-1)!} \int_0^\pi \frac{(\sin^{2K}\theta)K^K(M^2-1)^K}{3^K}d\theta$$

$$= \frac{2^{K-1}(M-1)(K-1)!}{M(2K-1)!}\left[\frac{K(M^2-1)}{3(\log_2 M)}\right]^K \frac{1}{\pi}\int_0^\pi \sin^{2K}\theta d\theta .$$

Using Lemma 2, we obtain:

$$\lambda_{b_K,M} = \frac{2^{K-1}(M-1)(K-1)!}{M(2K-1)!}\left[\frac{M^2-1}{3(\log_2 M)}\right]^K \frac{2^{-2K}\pi}{\pi}\frac{(2K)!}{K!K!}$$

$$= \frac{M-1}{M}\left[\frac{M^2-1}{6(\log_2 M)}\right]^K \frac{K^K}{K!} . \qquad\blacksquare$$

**MQAM signaling**

The asymptotic performance of MRC-MQAM is given by

$$\lambda_{b_K,M} = \left[\frac{M-1}{6(\log_2 M)}\right]^K \frac{(2K)!}{K!K!}\left(1-\frac{1}{M}\right) - \left[\frac{(M-1)}{6(\log_2 M)}\right]^K \frac{8}{\pi}\left(1-\frac{1}{\sqrt{M}}\right)^2 \sum_{l=0}^K \binom{2K}{K-l}\frac{\sin\frac{\pi l}{2}}{2l}$$

(3.24).

Proof:

According to Theorem 2,

$$\lambda_{K,M} = 1/(K-1)! \int_0^\infty p_e(\rho;M)\rho^{K-1}d\rho$$

From (2.12) we have

$$p_e(\rho;M) = 2\left(1 - \frac{1}{\sqrt{M}}\right)erfc\left(\sqrt{\frac{3\rho}{2(M-1)}}\right) - \left(1 - \frac{1}{\sqrt{M}}\right)^2 erfc^2\left(\sqrt{\frac{3\rho}{2(M-1)}}\right) \quad,$$

therefore

$$\lambda_{b_K,M} = \frac{1}{(K-1)!(\log_2 M)^K} \int_0^\infty \rho^{K-1} \left[ \begin{array}{c} 2\left(1 - \frac{1}{\sqrt{M}}\right)erfc\left(\sqrt{3\rho/2(M-1)}\right) \\ -\left(1 - \frac{1}{\sqrt{M}}\right)^2 erfc^2\left(\sqrt{3\rho/2(M-1)}\right) \end{array} \right] d\rho$$

From $erfc(y) = \frac{1}{\pi}\int_0^\pi d\theta \exp\left[\frac{-y^2}{\sin^2\theta}\right]$, $Q^2(y) = \frac{1}{\pi}\int_0^{\pi/4} d\theta \exp\left[\frac{-y^2}{2\sin^2\theta}\right]$ [11] [12],

and $2Q(\sqrt{2}y) = erfc(y)$ we have

$$\lambda_{b_K,M} = \frac{1}{(K-1)!(\log_2 M)^K} \int_0^\infty d\rho\rho^{K-1} \frac{2}{\pi}\left(1 - \frac{1}{\sqrt{M}}\right)\int_0^\pi d\theta \exp\left[\frac{-3\rho}{2(M-1)\sin^2\theta}\right]$$

$$- \frac{1}{(K-1)!(\log_2 M)^K} \int_0^\infty d\rho\rho^{K-1}\left(1 - \frac{1}{\sqrt{M}}\right)^2 \frac{4}{\pi}\int_0^{\pi/4} d\theta \exp\left[\frac{-3\rho}{2(M-1)\sin^2\theta}\right]$$

$$= \frac{2}{(\log_2 M)^K \pi}\left(1 - \frac{1}{\sqrt{M}}\right)\int_0^\pi d\theta \frac{1}{(K-1)!}\int_0^\infty d\rho\rho^{K-1} \exp\left[-\rho\frac{3}{2(M-1)\sin^2\theta}\right]$$

$$- \frac{4}{(\log_2 M)^K \pi}\left(1 - \frac{1}{\sqrt{M}}\right)^2 \int_0^{\pi/4} d\theta \frac{1}{(K-1)!}\int_0^\infty d\rho\rho^{K-1} \exp\left[-\rho\frac{3}{2(M-1)\sin^2\theta}\right].$$

Using Lemma 1, we obtain

$$\lambda_{b_K,M} = \frac{2}{(\log_2 M)^K \pi}\left(1 - \frac{1}{\sqrt{M}}\right)\int_0^\pi \frac{(\sin^{2K}\theta)2^K(M-1)^K}{3^K}d\theta$$

$$- \frac{4}{(\log_2 M)^K \pi}\left(1 - \frac{1}{\sqrt{M}}\right)^2 \int_0^{\pi/4} \frac{(\sin^{2K}\theta)2^K(M-1)^K}{3^K}d\theta$$

$$= \left[\frac{2(M-1)}{3(\log_2 M)}\right]^K\left(1 - \frac{1}{\sqrt{M}}\right)\frac{2}{\pi}\int_0^\pi \sin^{2K}\theta d\theta - \left[\frac{2(M-1)}{3(\log_2 M)}\right]^K\left(1 - \frac{1}{\sqrt{M}}\right)^2 \frac{4}{\pi}\int_0^{\pi/4} \sin^{2K}\theta d\theta$$

Using Lemma 2, we obtain:

45

$$\lambda_{b_K,M} = \left[\frac{2(M-1)}{3(\log_2 M)}\right]^K \frac{2^{-2K+1}\pi}{\pi} \frac{(2K)!}{K!K!}\left(1-\frac{1}{\sqrt{M}}\right) - \left[\frac{2(M-1)}{3(\log_2 M)}\right]^K \frac{2^{-2K+2}\pi}{4\pi} \frac{(2K)!}{K!K!}\left(1-\frac{1}{\sqrt{M}}\right)^2$$

$$-\left[\frac{2(M-1)}{3(\log_2 M)}\right]^K \frac{2^3}{2^{2K}\pi}\left(1-\frac{1}{\sqrt{M}}\right)^2 \sum_{l=0}^{K}\binom{2K}{K-l}\frac{\sin\frac{\pi l}{2}}{2l}$$

$$=\left[\frac{M-1}{6(\log_2 M)}\right]^K \frac{(2K)!}{K!K!}\left(1-\frac{1}{M}\right) - \left[\frac{(M-1)}{6(\log_2 M)}\right]^K \frac{8}{\pi}\left(1-\frac{1}{\sqrt{M}}\right)^2 \sum_{l=0}^{K}\binom{2K}{K-l}\frac{\sin\frac{\pi l}{2}}{2l} \blacksquare$$

The asymptotic performance of EGC-MQAM is given as

$$\lambda_{b_K,M} = \left[\frac{K(M-1)}{3(\log_2 M)}\right]^K \frac{1}{K!}\left(1-\frac{1}{M}\right) - \left[\frac{K(M-1)}{3(\log_2 M)}\right]^K \frac{4(K-1)!}{\pi(2K-1)!}\left(1-\frac{1}{\sqrt{M}}\right)^2 \sum_{l=0}^{K}\binom{2K}{K-l}\frac{\sin\frac{\pi l}{2}}{2l}$$

$$(3.25).$$

Proof:

According to Theorem 3, we have

$$\lambda_{K,M} = 2^{K-1}/(2K-1)! \int_0^\infty p_e(\rho_t;M)\rho_t^{K-1} d\rho_t$$

since

$$p_e(\rho_t;M) = 2\left(1-\frac{1}{\sqrt{M}}\right)erfc\left(\sqrt{\frac{3\rho_t}{2K(M-1)}}\right) - \left(1-\frac{1}{\sqrt{M}}\right)^2 erfc^2\left(\sqrt{\frac{3\rho_t}{2K(M-1)}}\right) \quad \text{and}$$

(3.19), therefore

$$\lambda_{b_K,M} = \frac{2^{K-1}}{(2K-1)!(\log_2 M)^K}\int_0^\infty \rho_t^{K-1}\left[\begin{array}{c} 2\left(1-\frac{1}{\sqrt{M}}\right)erfc\left(\sqrt{\frac{3\rho_t}{2K(M-1)}}\right) \\ -\left(1-\frac{1}{\sqrt{M}}\right)^2 erfc^2\left(\sqrt{\frac{3\rho_t}{2K(M-1)}}\right)\end{array}\right] d\rho_t$$

From $\quad erfc(y) = \frac{1}{\pi}\int_0^\pi d\theta \exp\left[\frac{-y^2}{\sin^2\theta}\right]$ , $\quad Q^2(y) = \frac{1}{\pi}\int_0^{\pi/4} d\theta \exp\left[\frac{-y^2}{2\sin^2\theta}\right]$

$2Q(\sqrt{2}y) = erfc(y)$ we have $erfc^2(y) = \frac{4}{\pi}\int_0^{\pi/4} d\theta \exp\left[\frac{-y^2}{\sin^2\theta}\right]$ . So

46

$$\lambda_{b_K,M} = \frac{2^K}{(2K-1)!(\log_2 M)^K} \int_0^\infty d\rho_t \rho_t^{K-1} \left(1 - \frac{1}{\sqrt{M}}\right) \frac{1}{\pi} \int_0^\pi d\theta \exp\left[\frac{-3\rho_t}{2K(M-1)\sin^2\theta}\right]$$

$$- \frac{2^{K-1}}{(2K-1)!(\log_2 M)^K} \int_0^\infty d\rho_t \rho_t^{K-1} \left(1 - \frac{1}{\sqrt{M}}\right)^2 \frac{4}{\pi} \int_0^{\pi/4} d\theta \exp\left[\frac{-3\rho_t}{2K(M-1)\sin^2\theta}\right]$$

$$= \frac{2^K(K-1)!}{(\log_2 M)^K \pi(2K-1)!} \left(1 - \frac{1}{\sqrt{M}}\right) \int_0^\pi d\theta \frac{1}{(K-1)!} \int_0^\infty d\rho_t \rho_t^{K-1} \exp\left[-\rho_t \frac{3}{2K(M-1)\sin^2\theta}\right]$$

$$- \frac{2^{K+1}(K-1)!}{(\log_2 M)^K \pi(2K-1)!} \left(1 - \frac{1}{\sqrt{M}}\right)^2 \int_0^{\pi/4} d\theta \frac{1}{(K-1)!} \int_0^\infty d\rho_t \rho_t^{K-1} \exp\left[-\rho_t \frac{3}{2K(M-1)\sin^2\theta}\right]$$

Using Lemma 1, we obtain

$$\lambda_{b_K,M} = \frac{2^K(K-1)!}{(\log_2 M)^K \pi(2K-1)!} \left(1 - \frac{1}{\sqrt{M}}\right) \int_0^\pi \frac{\sin^{2K}\theta (2K)^K (M-1)^K}{3^K} d\theta$$

$$- \frac{2^{K+1}(K-1)!}{(\log_2 M)^K \pi(2K-1)!} \left(1 - \frac{1}{\sqrt{M}}\right)^2 \int_0^{\pi/4} \frac{\sin^{2K}\theta (2K)^K (M-1)^K}{3^K} d\theta$$

$$= \frac{2^K(K-1)!}{(2K-1)!} \left[\frac{2K(M-1)}{3(\log_2 M)}\right]^K \left(1 - \frac{1}{\sqrt{M}}\right) \frac{1}{\pi} \int_0^\pi \sin^{2K}\theta d\theta$$

$$- \frac{2^{K+1}(K-1)!}{(2K-1)!} \left[\frac{2K(M-1)}{3(\log_2 M)}\right]^K \left(1 - \frac{1}{\sqrt{M}}\right)^2 \frac{1}{\pi} \int_0^{\pi/4} \sin^{2K}\theta d\theta$$

Using Lemma 2, we obtain:

$$\lambda_{b_K,M} = \left[\frac{2K(M-1)}{3(\log_2 M)}\right]^K \frac{2^K(K-1)!}{\pi(2K-1)!} \frac{2^{-2K}\pi(2K)!}{K!K!} \left(1 - \frac{1}{\sqrt{M}}\right)$$

$$- \left[\frac{2K(M-1)}{3(\log_2 M)}\right]^K \frac{2^{K+1}(K-1)!}{\pi(2K-1)!} \frac{2^{-2K}\pi(2K)!}{4K!K!} \left(1 - \frac{1}{\sqrt{M}}\right)^2$$

$$- \left[\frac{2K(M-1)}{3(\log_2 M)}\right]^K \frac{2^{K+2}(K-1)!}{2^{2K}\pi(2K-1)!} \left(1 - \frac{1}{\sqrt{M}}\right)^2 \sum_{l=0}^K \binom{2K}{K-l} \frac{\sin\frac{\pi l}{2}}{2l}$$

47

$$= \left[\frac{K(M-1)}{3(\log_2 M)}\right]^K \frac{1}{K!}\left(1-\frac{1}{M}\right) - \left[\frac{K(M-1)}{3(\log_2 M)}\right]^K \frac{4(K-1)!}{\pi(2K-1)!}\left(1-\frac{1}{\sqrt{M}}\right)^2 \sum_{l=0}^{K}\binom{2K}{K-l}\frac{\sin\frac{\pi l}{2}}{2l}$$

■

**MFSK signaling**

In the quadratic noncoherent receiver, the asymptotic parameter for MFSK with

$K = 1$ is [1]

$$\lambda_{b_1,M} = \frac{1}{\log_2 M}\sum_{m=1}^{M-1}\frac{1}{m} \quad. \tag{3.26}$$

Proof:

From Theorem 2, $\lambda_{K,M} = \frac{1}{(K-1)!}\int_0^\infty p_e(\rho;M)\rho^{K-1}d\rho$. When $K = 1$

$$\lambda_{1,M} = \int_0^\infty p_e(\rho;M)d\rho$$

since $p_e(\rho_0;M) = \sum_{m=1}^{M-1}\frac{(-1)^{m+1}}{m+1}\binom{M-1}{m}\exp\left[\frac{-m\rho_0}{m+1}\right]$,

$\lambda_{b_1,M} = \dfrac{\lambda_{1,M}}{\log_2 M}$ we obtain:

$$\lambda_{b_1,M} = \frac{1}{\log_2 M}\int_0^\infty \sum_{m=1}^{M-1}\frac{(-1)^{m+1}}{m+1}\binom{M-1}{m}\exp\left[\frac{-m\rho}{m+1}\right]d\rho$$

$$= \frac{1}{\log_2 M}\sum_{m=1}^{M-1}\frac{(-1)^{m+1}}{m+1}\binom{M-1}{m}\left[\frac{m+1}{m}\right]$$

$$= \frac{1}{\log_2 M}\sum_{m=1}^{M-1}\frac{(-1)^{m+1}}{m}\binom{M-1}{m}.$$

Since $\displaystyle\sum_{k=1}^{n}\frac{(-1)^{k+1}}{k}\binom{n}{k} = \sum_{m=1}^{n}\frac{1}{m}$ [13] , we obtain

$$\lambda_{b_1,M} = \frac{1}{\log_2 M}\sum_{m=1}^{M-1}\frac{1}{m}.$$

■

48

In the matched filter coherent receiver, for $K = 1$ M-ary orthogonal signaling

the asymptotical parameter for MFSK with $K = 1$ is [1]

$$\lambda_{b_1,M} = \frac{M-1}{M\log_2 M} + \frac{2}{\log_2 M}\int_{-\infty}^{\infty} y\left[\frac{erfc(-y)}{2} - \left(\frac{erfc(-y)}{2}\right)^M\right]dy. \quad (3.27)$$

Proof:

From Theorem 2, $\lambda_{K,M} = \frac{1}{(K-1)!}\int_0^{\infty} p_e(\rho;M)\rho^{K-1}d\rho$ . When $K = 1$, we have

$$\lambda_{1,M} = \int_0^{\infty} p_e(\rho;M)d\rho$$

Since $p_e(\rho,M) = \frac{1}{\sqrt{\pi}}\int_{-\infty}^{\infty} e^{-(y-\sqrt{\rho})^2}\left[1 - \left(\frac{1}{2}erfc(-y)\right)^{M-1}\right]dy$ , we have

$$\lambda_{b_1,M} = \frac{\lambda_{1,M}}{\log_2 M} = \frac{1}{\log_2 M}\int_0^{\infty} d\rho\frac{1}{\sqrt{\pi}}\int_{-\infty}^{\infty} dy e^{-(y-\sqrt{\rho})^2}\left[1 - \left(\frac{1}{2}erfc(-y)\right)^{M-1}\right]$$

$$= \frac{1}{\sqrt{\pi}\log_2 M}\int_{-\infty}^{\infty} dy\left[1 - \left(\frac{1}{2}erfc(-y)\right)^{M-1}\right]\int_0^{\infty} d\rho e^{-(y-\sqrt{\rho})^2} .$$

Assuming $t = y - \sqrt{\rho}$ , we have

$$\lambda_{b_1,M} = \frac{1}{\sqrt{\pi}\log_2 M}\int_{-\infty}^{\infty} dy\left[1 - \left(\frac{1}{2}erfc(-y)\right)^{M-1}\right]\int_y^{\infty} e^{-t^2}(2tdt - 2ydt)$$

$$= \frac{1}{\sqrt{\pi}\log_2 M}\int_{-\infty}^{\infty} dy\left[1 - \left(\frac{1}{2}erfc(-y)\right)^{M-1}\right][e^{-y^2} + \sqrt{\pi}yerfc(-y)]$$

$$= \frac{1}{\sqrt{\pi}\log_2 M}\int_{-\infty}^{\infty} dy\left[e^{-y^2} - e^{-y^2}\left(\frac{1}{2}erfc(-y)\right)^{M-1} + \sqrt{\pi}yerfc(-y) - \sqrt{\pi}y\left(\frac{1}{2}erfc(-y)\right)^M\right].$$

Since $erfc(y) = \frac{2}{\sqrt{\pi}}\int_y^{\infty} e^{-t^2}dt$ , we have $d\left(\frac{1}{2}erfc(-y)\right) = e^{-y^2}/\sqrt{\pi}dy$ . Therefore,

$$\lambda_{b_1,M} = \frac{1}{\log_2 M} - \frac{1}{\log_2 M}\int_{-\infty}^{\infty} d\left(\frac{1}{2}erfc(-y)\right)\left(\frac{1}{2}erfc(-y)\right)^{M-1} + \frac{2}{\log_2 M}\int_{-\infty}^{\infty} y\left[\frac{erfc(-y)}{2} - \left(\frac{1}{2}erfc(-y)\right)^M\right],$$

49

Assuming $x = \dfrac{1}{2} erfc(-y)$ ,

$$\lambda_{b_1,M} = \frac{1}{\log_2 M} - \frac{1}{\log_2 M} \int_0^1 x^{M-1} dx + \frac{2}{\log_2 M} \int_{-\infty}^{\infty} y \left[ \frac{erfc(-y)}{2} - \left( \frac{1}{2} erfc(-y) \right)^M \right] dy$$

$$= \frac{1}{\log_2 M} - \frac{1}{M \log_2 M} x^M \Big|_0^1 + \frac{2}{\log_2 M} \int_{-\infty}^{\infty} y \left[ \frac{erfc(-y)}{2} - \left( \frac{1}{2} erfc(-y) \right)^M \right] dy$$

$$= \frac{M-1}{M \log_2 M} + \frac{2}{\log_2 M} \int_{-\infty}^{\infty} y \left[ \frac{erfc(-y)}{2} - \left( \frac{erfc(-y)}{2} \right)^M \right] dy \qquad \blacksquare$$

The results we have obtained in this chapter are summarized in Table I.

50

Table I Asymptotic Parameters for M-ary Signaling on Rician fading channels

| Signaling and Receiver Schemes | Asymptotic Parameter $\lambda_{b_K,M}$ |
|---|---|
| MRC-MPSK | $$\frac{2^{-2K}}{[\log_2 M \sin^2(\pi/M)]^K}\left[\binom{2K}{K}\left(\frac{M-1}{M}\right)-\sum_{l=1}^{K}\binom{2K}{K-l}(-1)^l\frac{\sin(2\pi l/M)}{\pi l}\right]$$ |
| EGC-MPSK | $$\frac{(K/2)^K K!}{(2K)![\log_2 M \sin^2(\pi/M)]^K}\left[\binom{2K}{K}\left(\frac{M-1}{M}\right)-\sum_{l=1}^{K}\binom{2K}{K-l}(-1)^l\frac{\sin(2\pi l/M)}{\pi l}\right]$$ |
| MRC-MPAM | $$\frac{M-1}{M}\left[\frac{M^2-1}{12\log_2 M}\right]^K\binom{2K}{K}$$ |
| EGC-MPAM | $$\frac{M-1}{M}\left[\frac{M^2-1}{6\log_2 M}\right]^K\frac{K^K}{K!}$$ |
| MRC-MQAM | $$\lambda_{b_K,M}=\left[\frac{M-1}{6(\log_2 M)}\right]^K\frac{(2K)!}{K!K!}\left(1-\frac{1}{M}\right)$$ $$-\left[\frac{(M-1)}{6(\log_2 M)}\right]^K\frac{8}{\pi}\left(1-\frac{1}{\sqrt{M}}\right)^2\sum_{l=0}^{K}\binom{2K}{K-l}\frac{\sin\frac{\pi l}{2}}{2l}$$ |
| EGC-MQAM | $$\lambda_{b_K,M}=\left[\frac{K(M-1)}{3(\log_2 M)}\right]^K\frac{1}{K!}\left(1-\frac{1}{M}\right)$$ $$-\left[\frac{K(M-1)}{3(\log_2 M)}\right]^K\frac{4(K-1)!}{\pi(2K-1)!}\left(1-\frac{1}{\sqrt{M}}\right)^2\sum_{l=0}^{K}\binom{2K}{K-l}\frac{\sin\frac{\pi l}{2}}{2l}$$ |
| NonCoh-MFSK | $$\frac{1}{\log_2 M}\sum_{n=1}^{M-1}\frac{1}{n}\quad(K=1)$$ |
| MF-MFSK | $$\frac{M-1}{M\log_2 M}+\frac{2}{\log_2 M}\int_{-\infty}^{\infty}dy\,y\left[\frac{erfc(-y)}{2}-\left(\frac{erfc(-y)}{2}\right)^M\right]\quad(K=1)$$ |

51

## 3.5 Asymptotic Performance on Multipath Rayleigh Fading Channels

For the Rayleigh fading channel, the asymptotic SER is given by [1]

$$P_e(K,M) = \frac{\lambda_{K,M}}{\Gamma_{K,M}}. \tag{3.28}$$

Proof:

Based on (3.9) $P_e(K;M) = \dfrac{e^{-\Delta_k}\lambda_{K,M}}{\Gamma_{K,M}}$ . For the Rayleigh channel $\Delta_k = 0$ we have

$$P_e(K;M) = \frac{e^{-\Delta_k}\lambda_{K,M}}{\Gamma_{K,M}} = e^0 \frac{\lambda_{K,M}}{\Gamma_{K,M}} = \frac{\lambda_{K,M}}{\Gamma_{K,M}}. \qquad \blacksquare$$

## 3.6 Numerical Results

In the following simulations, for multipath Rician fading channel, it is assumed that $v_k^2 = 10$ and $2\sigma_k^2 = 30$, with $v_k^2$ and $2\sigma_k^2$ defined in (3.4). It is also assumed that the average SNR $E/N_0$, which is also defined in (3.4), is equal to 1. For multipath Rayleigh fading channel, it is assumed that $2\sigma_k^2 = 40$, so that the total energy in multipaths of the Rayleigh fading channel and the Rician fading channel is the same and we can provide a fair comparison between these two channels. All the other settings are kept the same as in the multipath Rician fading channel case.

Figure 3.2 shows the asymptotic SER of MPSK, MPAM and MQAM signaling with coherent MRC receiver in the multipath Rician fading channel under different diversity order $K$. We notice that as $K$ increases, the asymptotic SER decreases, i.e., the performance becomes better as diversity order increases. In addition, from the

curves, it can be shown that MQAM is better than MPSK, and MPSK is better than MPAM in terms of the asymptotic SER performance. As expected, as the modulation constellation size $M$ increases, the performance degrades.

The asymptotical SER of MPSK, MPAM and MQAM signaling with coherent EGC receiver in the multipath Rician fading channel under different diversity order is given in Figure 3.3. From this figure, similar conclusions as discussed above in Figure 3.2 can be drawn. That is, the asymptotic SER of MQAM is superior to that of MPSK, and the asymptotic SER of MPSK is better than that of MPAM.

We also compare the asymptotical SER of MPSK, MPAM and MQAM signaling with MRC and EGC receivers in the multipath Rician fading channel in Figure 3.4. The results in Figure 3.4 confirm the well-known conclusion that MRC provides a better performance than EGC.

For the multipath Rayleigh fading channel, the asymptotical SERs of MPSK, MPAM and MQAM signaling with coherent MRC receiver and coherent EGC receiver under different diversity order are given in Figures 3.5 and 3.6, respectively. From these figures, similar conclusions as discussed above in Figures 3.2 and 3.3 can be drawn. That is, the asymptotic SER of MQAM is superior to that of MPSK, and the asymptotic SER of MPSK is better than that of MPAM.

In Figure 3.7, we compare the asymptotical SER of MPSK, MPAM and MQAM signaling with MRC receivers in the multipath Rayleigh and the multipath Rician fading channels, and in Figure 3.8 we compare that with EGC receivers. The results in

53

Figures 3.7 and 3.8 show that Rician fading channels provide a little bit better performance than Rayleigh fading channels.

The asymptotical SER of MFSK with single received branch and with coherent and non-coherent receivers under different values of modulation constellation size $M$ is given in Figure 3.9. The performance increases as $M$ improves. However, as $M$ becomes large, the impact of the increase in $M$ on the performance becomes less.
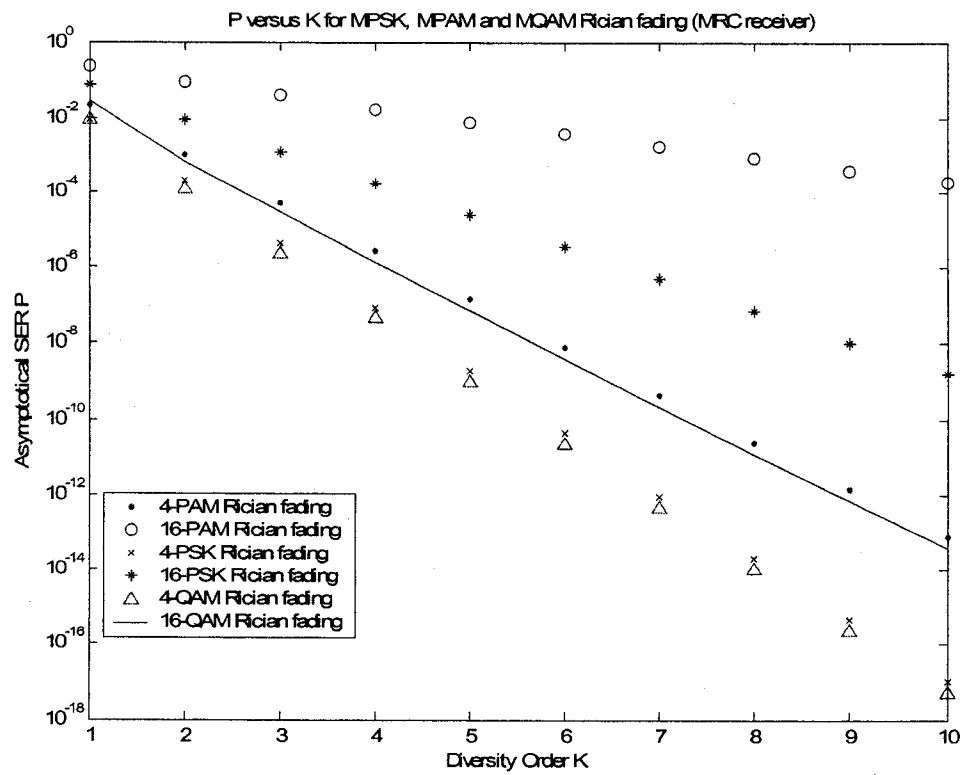
54

Figure 3.2 Asymptotical SER vs diversity order for MPSK, MPAM and MQAM
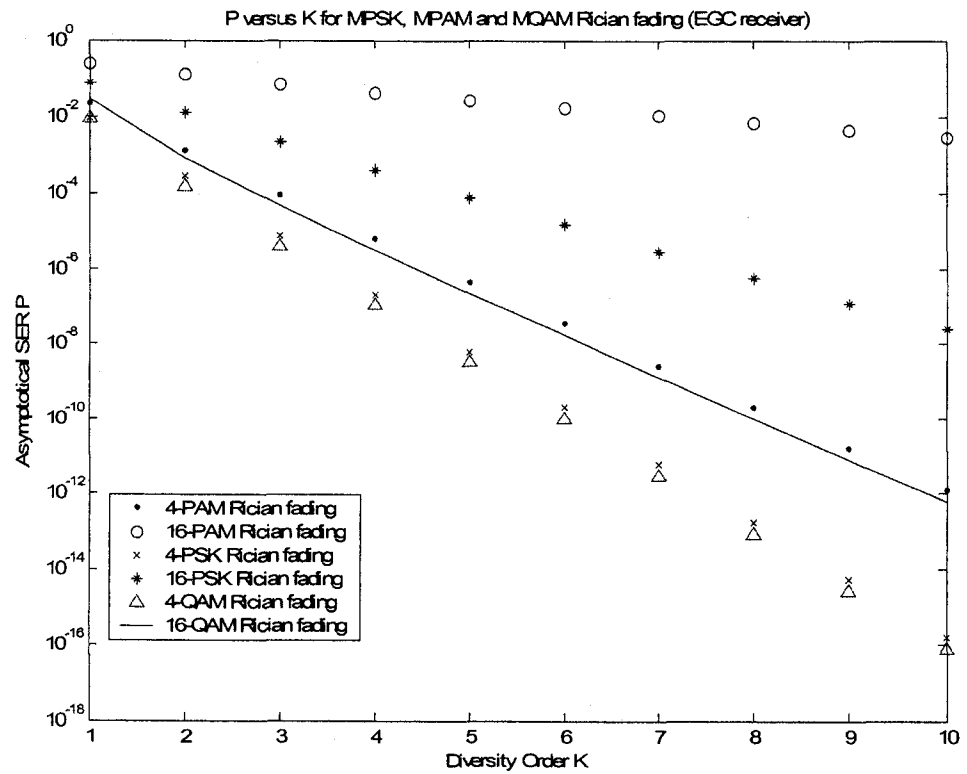Rician fading with MRC receiver

55

Figure 3.3 Asymptotical SER vs diversity order for MPSK, MPAM and MQAM
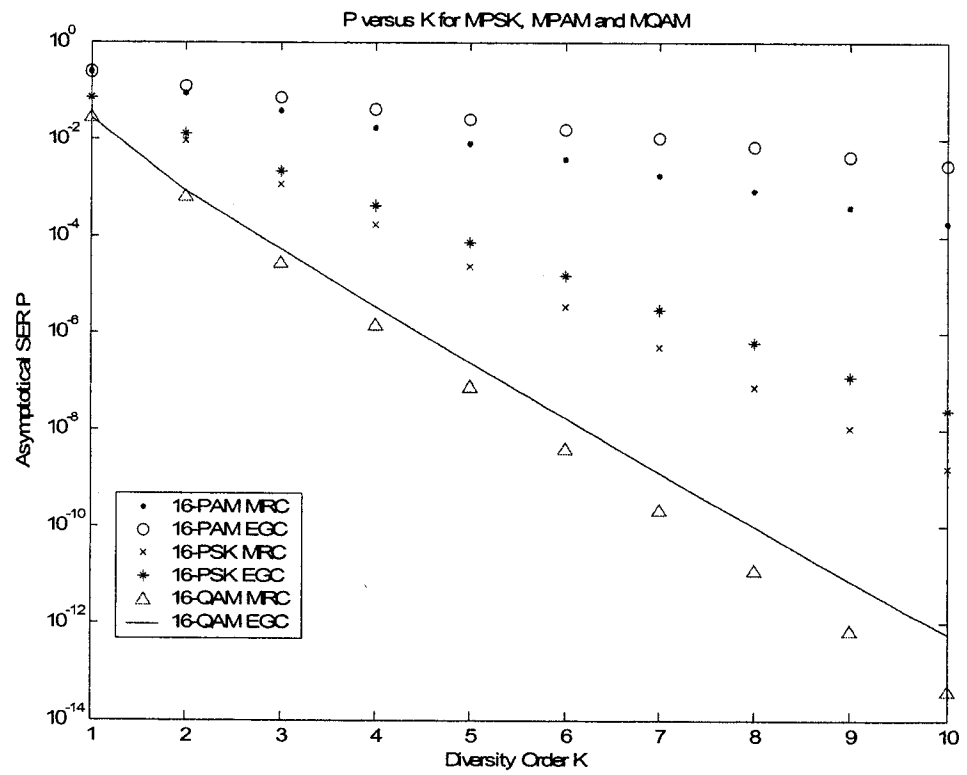Rician fading with EGC receiver

56

Figure 3.4 Asymptotical SER vs diversity order for MPSK, MPAM and MQAM
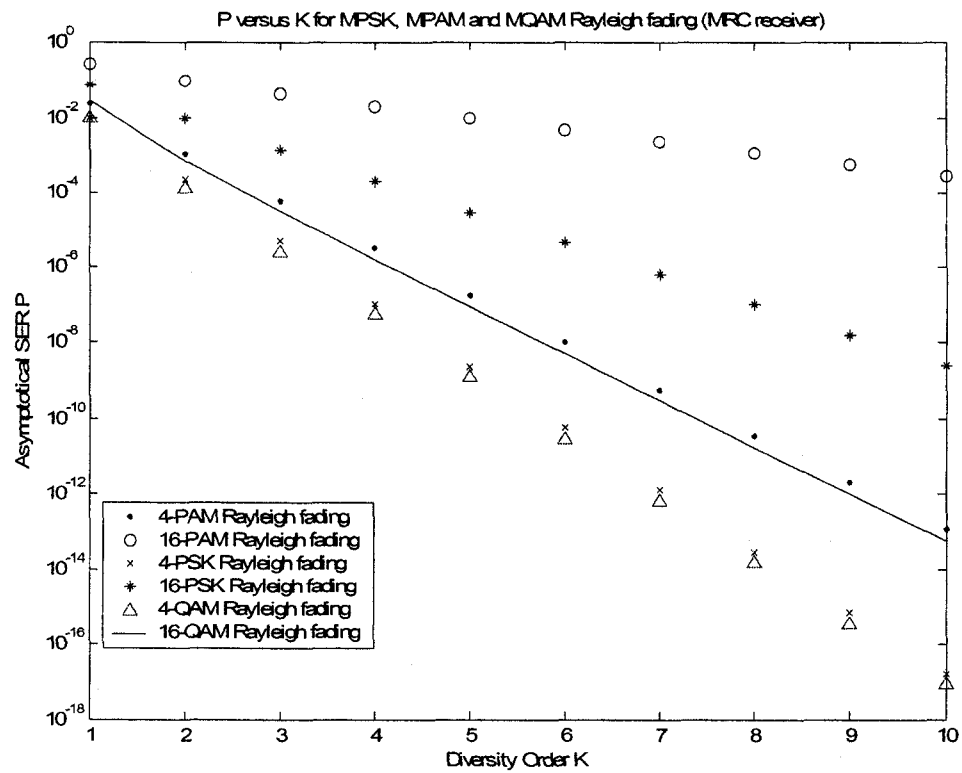Rician fading with MRC and EGC receiver

57

Figure 3.5 Asymptotical SER vs diversity order for MPSK, MPAM and MQAM
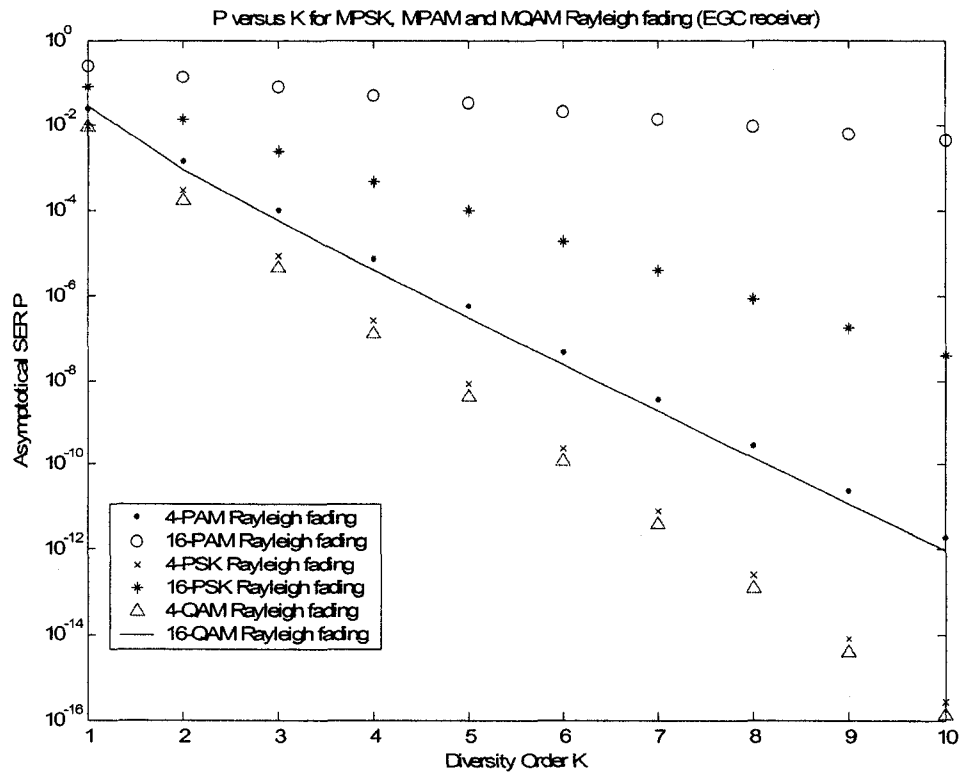Rayleigh fading with MRC receiver

58

Figure 3.6 Asymptotical SER vs diversity order for MPSK, MPAM and MQAM
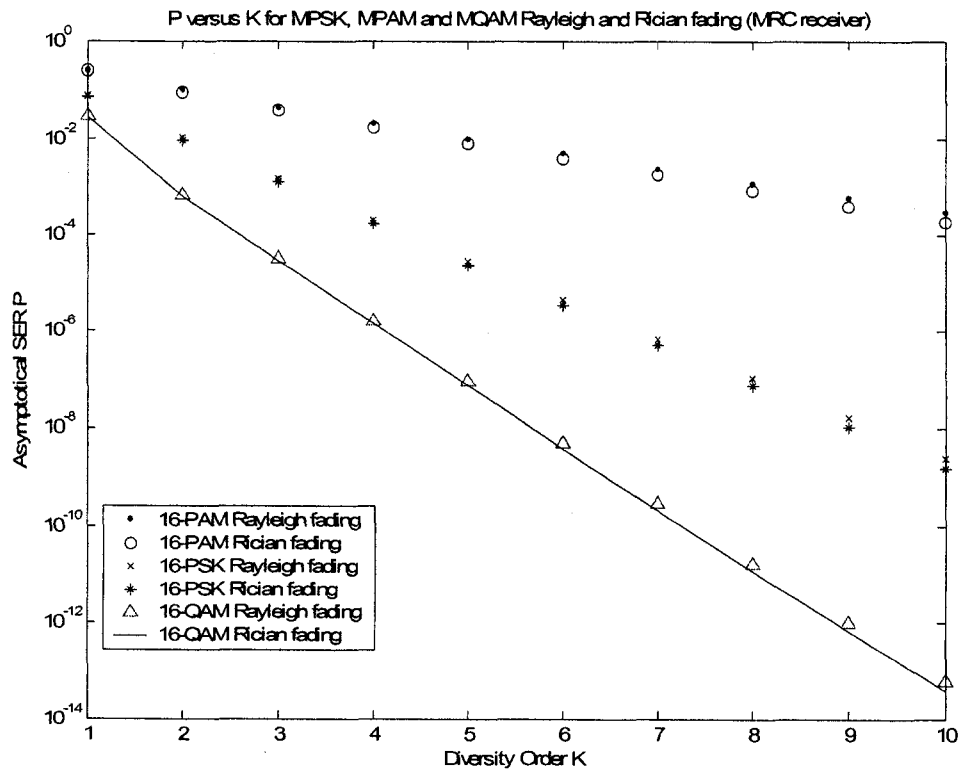Rayleigh fading with EGC receiver

59

Figure 3.7 Asymptotical SER vs diversity order for MPSK, MPAM and MQAM
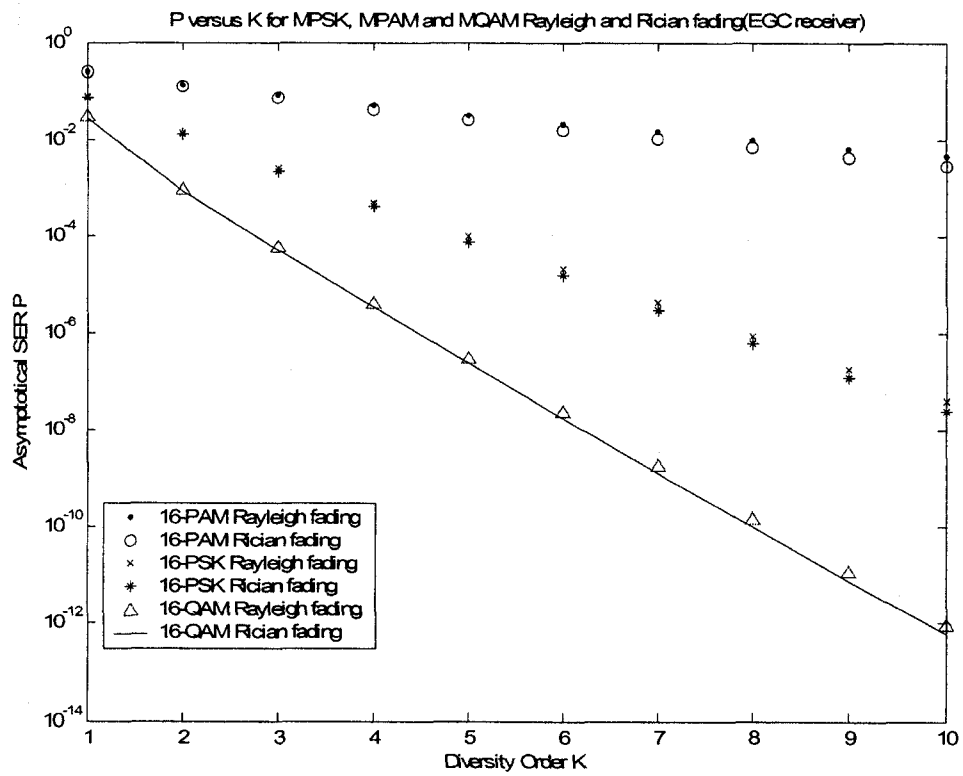Rayleigh and Rician fading with MRC receiver

60

Figure 3.8 Asymptotical SER vs diversity order for MPSK, MPAM and MQAM
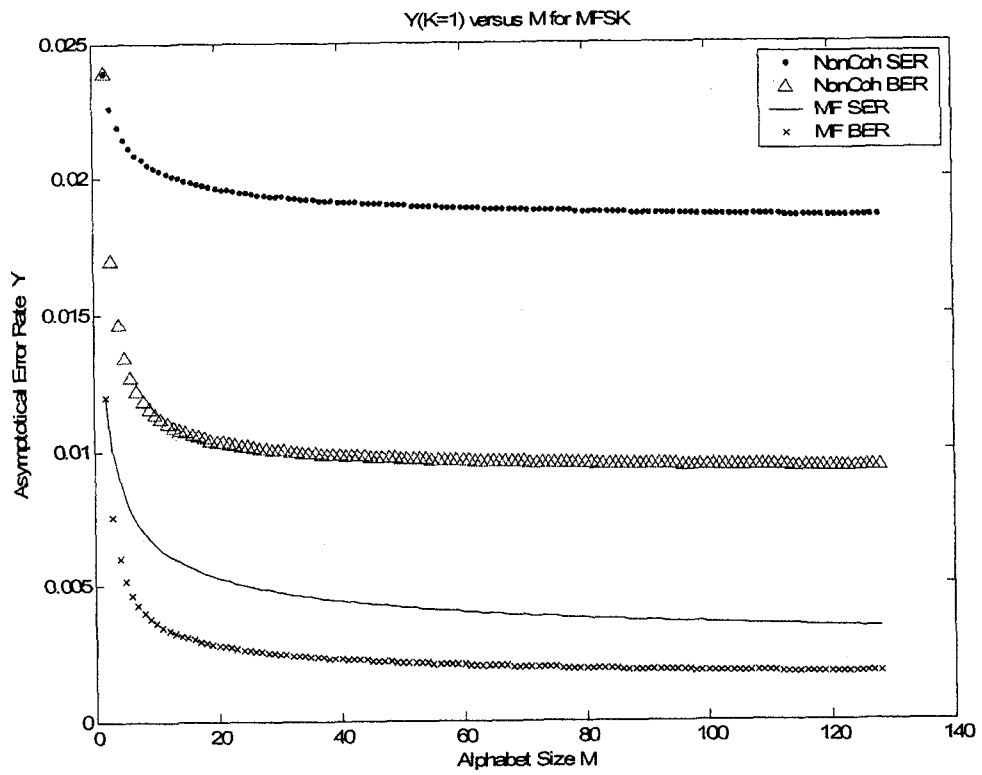Rayleigh and Rician fading with EGC receiver

61

Figure 3.9 Asymptotical SER of MFSK with coherent and non-coherent receivers under different M values

62

# Chapter 4

# Asymptotic Performance of OFDM M-ary Signals on Multipath Rician Fading Diversity Channels

In this chapter, based on the results obtained in Chapter 3, asymptotic performance of OFDM M-ary signals on multipath Rician fading diversity channels will be discussed.

## 4.1 System Model

We consider an OFDM system with N subcarriers. Denoting the modulated data sequence in one OFDM symbol as $D(0)$, $D(1)$, ..., $D(N-1)$, after the inverse discrete Fourier transform (IDFT), the time-domain OFDM signal can be expressed as [14]

$$S(n) = \frac{1}{N} \sum_{m=0}^{N-1} D(m) e^{j2\pi mn/N}, n = 0,1,...,N-1. \tag{4.1}$$

The channel impulse response of the multipath fading channel is modeled as a finite impulse response (FIR) filter with taps $h(n), n = 0,1,...,L-1$, where $L$ is the number of multipaths and $L \ll N$. $h(n), n = 0,1,...,L-1$ are mutually independent and can be written as

$$h(n) = |h(n)| e^{j\phi_n} = r_n e^{j\phi_n} . \tag{4.2}$$

The joint PDF of $r_n$ and $\phi_n$ for a multipath Rician fading channel is given by [15]

63

$$f_{R_n,\Phi_n}(r_n,\phi_n) = \frac{r_n}{2\pi\sigma^2}\exp\left[-\frac{r_n^2 + r_{sn}^2 - 2r_n r_{sn}\cos\phi_n}{2\sigma^2}\right] \tag{4.3}$$

where $r_{sn}$ is the dominant component of the nth channel tap, and $\sigma^2$ is the variance.

Therefore, the frequency-domain channel impulse response is [14]

$$H(m) = \sum_{n=0}^{N-1} h(n)e^{-j2\pi nm/N} = \sum_{n=0}^{L-1} h(n)e^{-j2\pi nm/N}. \tag{4.4}$$

It is assumed that the maximum delay is less than the length of the cyclic prefix, and perfect timing and synchronization are achieved at the receiver. Therefore, intersymbol interference (ISI) and inter-carrier interference (ICI) are not considered in the following analysis.

The received signal $r(n), n = 0,1,...,N-1$, is first analog-to-digital (A/D) processed and removed of the cyclic prefix. After the discrete Fourier transform (DFT), the output signal is given as

$$R(m) = \frac{1}{N}\sum_{n=0}^{N-1} r(n)e^{-j2\pi nm/N} = H(m)D(m) + N(m), m = 0,1,...,N-1 \tag{4.5}$$

where $N(m)$ are independent identically distributed (i.i.d.) complex Gaussian noise with zero mean and unit variance. That is, each OFDM subcarrier undergoes a frequency flat fading channel characterized by $H(m)$.

It is noted that

$$H(m) = \sum_{n=0}^{L-1} r_n e^{+j\phi_n} e^{-j2\pi nm/N} = \sum_{n=0}^{L-1} r_n e^{+j(\phi_n - 2\pi nm/N)} = \sum_{n=0}^{L-1} r_n e^{j\theta_n}$$

$$= \sum_{n=0}^{L-1} X_n + jY_n = X + jY \tag{4.6}$$

i.e., $\theta_n = \phi_n - 2\pi nm/N(\text{mod}\,2\pi)$. So the joint PDF of $r_n$ and $\theta_n$ is

$$f_{R_n,\Theta_n}(r_n,\theta_n) = \frac{r_n}{2\pi\sigma^2}\exp\left[-\frac{r_n^2 + r_{sn}^2 - 2r_n r_{sn}\cos(\theta_n + 2\pi nm/N)}{2\sigma^2}\right] \tag{4.7}$$

64

$$= \frac{r_n}{2\pi\sigma^2} \exp\left[ -\frac{1}{2\sigma^2} \left( r_n^{\ 2} + r_{sn}^{\ 2} - 2r_n r_{sn} \cos\theta_n \cos\frac{2\pi n m}{N} + 2r_n r_{sn} \sin\theta_n \sin\frac{2\pi n m}{N} \right) \right]$$

Define $X_n + jY_n = R_n e^{j\Theta_n}$ , so we have $X_n = R_n \cos\Theta_n$ , $Y_n = R_n \sin\Theta_n$ .

Also define $r_{sn}\cos\dfrac{2\pi n m}{N} = r_{sn}^{\ x}$ , $r_{sn}\sin\dfrac{2\pi n m}{N} = r_{sn}^{\ y}$ , then it can be show that the joint PDF of $X_n$ and $Y_n$ is

$$f_{X_n,Y_n}(x_n, y_n) = \frac{1}{2\pi\sigma^2}\exp\left( -\frac{x_n^{\ 2} + y_n^{\ 2} + r_{sn}^{\ 2} + 2y_n r_{sn}^{\ y} - 2x_n r_{sn}^{\ x}}{2\sigma^2} \right)$$

$$= \frac{1}{2\pi\sigma^2}\exp\left( -\frac{\left(x_n - r_{sn}^{\ x}\right)^2 + \left(y_n + r_{sn}^{\ y}\right)^2}{2\sigma^2} \right) \qquad (4.8)$$

By integrating over $y_n$ (or $x_n$ ), the PDF of $X_n$ (or $Y_n$ ) can be obtained. It can be shown that $X_n$ and $Y_n$ are independent Gaussian random variables. and

$X_n \sim N\!\left(r_{sn}^{\ x}, \sigma^2\right)$, $\qquad Y_n \sim N\!\left(-r_{sn}^{\ y}, \sigma^2\right)$ , with $N(.)$ representing Gaussian distribution.

From (4.6), we have $X = \sum\limits_{n=0}^{L-1} X_n$ , $Y = \sum\limits_{n=0}^{L-1} Y_n$ . Since the channel tap coefficients are independent, $X_0,...,X_{L-1}$ are mutually independent, $Y_0,...,Y_{L-1}$ are mutually independent, and $X_n$ and $Y_n$ $(n=0,1,...,L-1)$ are also mutually independent. So we have

$$X \sim N\!\left(r_{s0}^{\ x} + r_{s1}^{\ x} + ... + r_{s,L-1}^{\ x}, L\sigma^2\right) \qquad (4.9)$$

$$Y \sim N\!\left(-\left(r_{s0}^{\ y} + r_{s1}^{\ y} + ... + r_{s,L-1}^{\ y}\right), L\sigma^2\right) \qquad (4.10)$$

and X and Y are also mutually independent.

Let

$$r_{s0}^{\ x} + ... + r_{s,L-1}^{\ x} = r_{sx} \qquad (4.11)$$

$$r_{s0}^{\ y} + ... + r_{s,L-1}^{\ y} = r_{sy} \qquad (4.12)$$

65

$$r_s = \sqrt{r_{sx}^2 + r_{sy}^2} \tag{4.13}$$

then

$$|H(k)| \sim Rice\left(\sqrt{r_{sx}^2 + r_{sy}^2}, L\sigma^2\right) = Rice\left(r_s, L\sigma^2\right) \tag{4.14}$$

with $Rice(.)$ denoting Rician distribution. That is, we have

$$f_{|H(m)|}(r) = \frac{r}{L\sigma^2}\exp\left(-\frac{r^2 + r_s^2}{2L\sigma^2}\right)I_0\left(\frac{rr_s}{L\sigma^2}\right) \tag{4.15}$$

## 4.2 Asymptotic Performance of OFDM Signaling

Suppose that there are K diversity branches at OFDM receiver. Based on the discussion in 4.1 and in Chapter 3, we have

$$P_k = r_{s,k}^2 E / N_0 \tag{4.16}$$

$$\gamma_k = 2L\sigma_k^2 E / N_0 \tag{4.17}$$

where $r_{s,k}$ is obtained according to (4.13).

Then $\delta_k = \dfrac{P_k}{\gamma_k} = \dfrac{r_{s,k}^2}{2L\sigma^2}$ , $\Delta_k = \displaystyle\sum_{k=0}^{K-1}\delta_k$ , and $\Gamma_{K,M} = \displaystyle\prod_{k=0}^{K-1}\gamma_k$ . Therefore

according to the discussion in Chapter 3, we have

$$P_{e_{asy}}(K,M) = \frac{e^{-\Delta_k}\lambda_{K,M}}{\Gamma_{K,M}}$$

Therefore, the asymptotic SER of OFDM signals with diversity receiver can be calculated following the procedures listed below:

Step 1. For the $k$ th diversity branch, calculate

$$\begin{cases} r_{s,n}^x(k,m) = r_{s,n}(k)\cos\left(\dfrac{2\pi nm}{N}\right) \\ r_{s,n}^y(k,m) = r_{s,n}(k)\sin\left(\dfrac{2\pi nm}{N}\right) \end{cases}$$

$$\begin{cases} r_{sx}(k,m) = r_{s,0}^x(k,m) + \ldots + r_{s,L-1}^x(k,m) \\ r_{sy}(k,m) = r_{s,0}^y(k,m) + \ldots + r_{s,L-1}^y(k,m) \end{cases}$$

66

$$r_s(k,m) = \sqrt{r_{sx}^2(k,m) + r_{sy}^2(k,m)}$$

with $r_{s,n}(k,m)$ being the dominant component of the nth path on the $k$ th diversity branch and $m$ th subcarrier.

Step 2. Calculate

$$\delta_k^m = \frac{P_k^m}{\gamma_k} = \frac{r_s^2(k,m)}{2L\sigma^2}$$

$$\Delta_K^m = \sum_{k=0}^{K-1} \delta_k^m$$

$$\Gamma_{K,M} = \prod_{k=0}^{K-1} \gamma_k = (2L\sigma^2)^K$$

Step 3. Calculate $\lambda_{K,M}$ according to Table I in Chapter 3.

Step 4. $P_{e_{asy}}(K;M;m) = \dfrac{e^{-\Delta_K^m} \lambda_{K,M}}{\Gamma_{K,M}}$

Step 5. Find the average asymptotic SER over N subcarriers by

$$P_{e_{asy}}(K;M) = \frac{1}{N} \sum_{m=0}^{N-1} P_{e_{asy}}(K;M;m)$$

## 4.3 Numerical Results

In the following simulations, it is assumed that $L = 2$ and $E/N_0 = 1/L$. For multipath Rician fading channel, it is assumed that $r_{s,n}^2(k) = 10$ and $2\sigma_n^2(k) = 30$ ($n = 0,...,L-1$), with $r_{s,n}^2(k)$ defined in (4.16) and $2\sigma_n^2(k)$ defined in (4.17). For multipath Rayleigh fading channel, it is assumed that $2\sigma^2(k) = 40$ so that the total energy in multipaths of the Rayleigh fading channel and the Rician fading channel is the same and we can provide a fair comparison between these two channels. All the other settings are kept the same as in the multipath Rician fading

67

channel case.

Figure 4.1 shows the asymptotic SER of MPSK,MPAM and MQAM OFDM signals with coherent MRC receiver in the multipath Rician fading channel under different diversity order $K$. We notice that as $K$ increases, the asymptotic SER decreases, i.e., the performance becomes better as diversity order increases. In addition, from the curves, it can be shown that MQAM is better than MPSK, and MPSK is better than MPAM in terms of the asymptotic SER performance. As expected, as the modulation constellation size $M$ increases, the performance degrades.

The asymptotical SER of MPSK, MPAM and MQAM OFDM signals with coherent EGC receiver in the multipath Rician fading channel under different diversity order is given in Figure 4.2. From this figure, similar conclusions as discussed above in Figure 4.1 can be drawn. That is, the asymptotic SER of MQAM is superior to that of MPSK, and the asymptotic SER of MPSK is better than that of MPAM.

We also compare the asymptotical SER of MPSK, MPAM and MQAM OFDM signals with MRC and EGC receivers in the multipath Rician fading channel in Figure 4.3. The results in Figure 4.3 confirm the well-known conclusion that MRC provides a better performance than EGC.

For the multipath Rayleigh fading channel, the asymptotical SERs of MPSK, MPAM and MQAM OFDM signals with coherent MRC receiver and coherent EGC

receiver under different diversity order are given in Figures 4.4 and 4.5, respectively. From these figures, similar conclusions as discussed above in Figures 4.1 and 4.2 can be drawn. That is, the asymptotic SER of MQAM is superior to that of MPSK, and the asymptotic SER of MPSK is better than that of MPAM.

In Figure 4.6, we compare the asymptotical SER of MPSK, MPAM and MQAM OFDM signals with MRC receivers in the multipath Rayleigh and the multipath Rician fading channels, and in Figure 4.7 we compare that with EGC receivers. The results in Figures 4.6 and 4.7 show that Rician fading channels provide better performance than Rayleigh fading channels.

Asymptotical SERs vs diversity order for MPSK, MPAM and MQAM single carrier and OFDM signals with MRC receiver and EGC receiver are given in Figure 4.8 and 4.9, respectively. It can be shown that OFDM systems outperform single carrier systems.
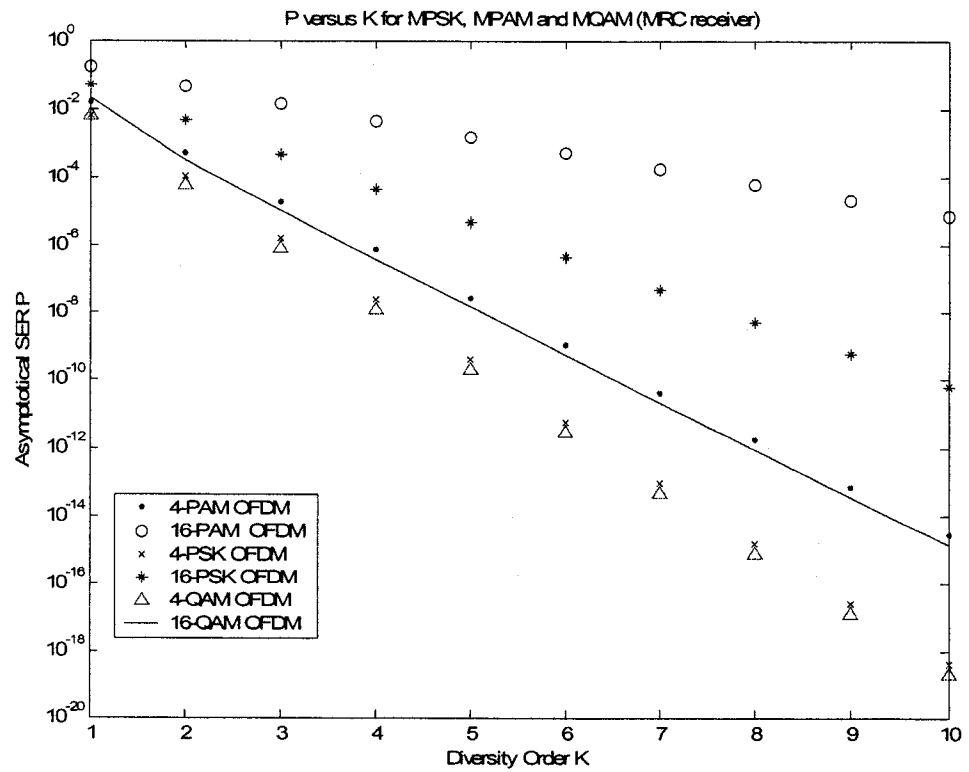
Figure 4.1 Asymptotical SER vs diversity order for MPSK, MPAM and MQAM of OFDM Rician fading with MRC receiver
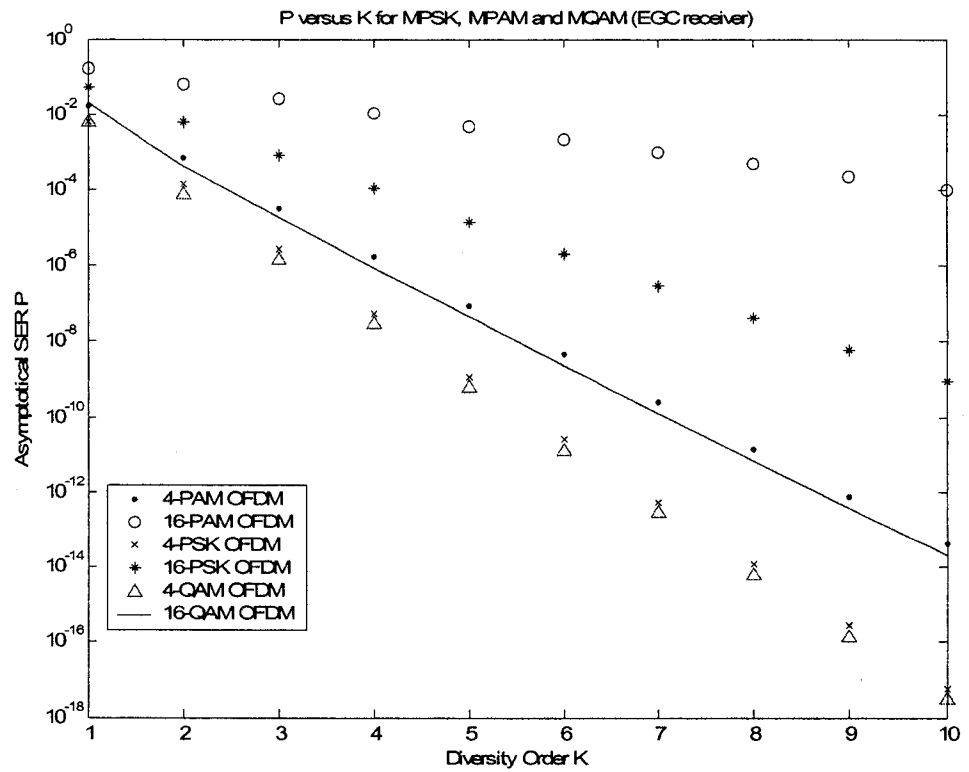
70

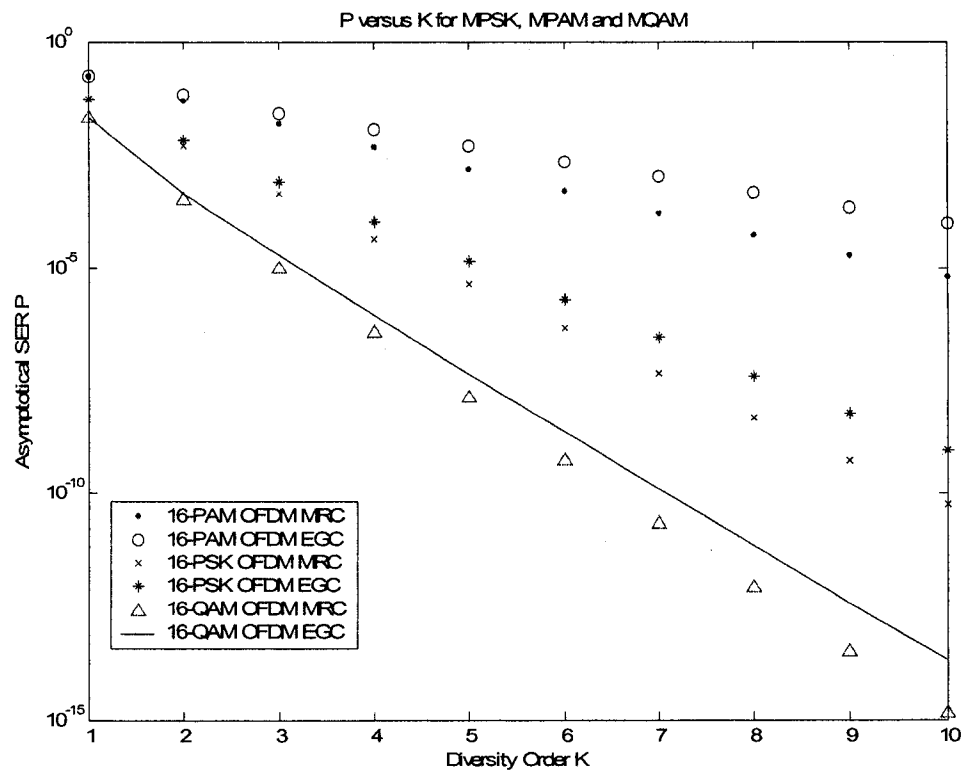Figure 4.2 Asymptotical SER vs diversity order for MPSK, MPAM and MQAM of OFDM Rician fading with EGC receiver

71

Figure 4.3 Asymptotical SER vs diversity order for MPSK, MPAM and MQAM of
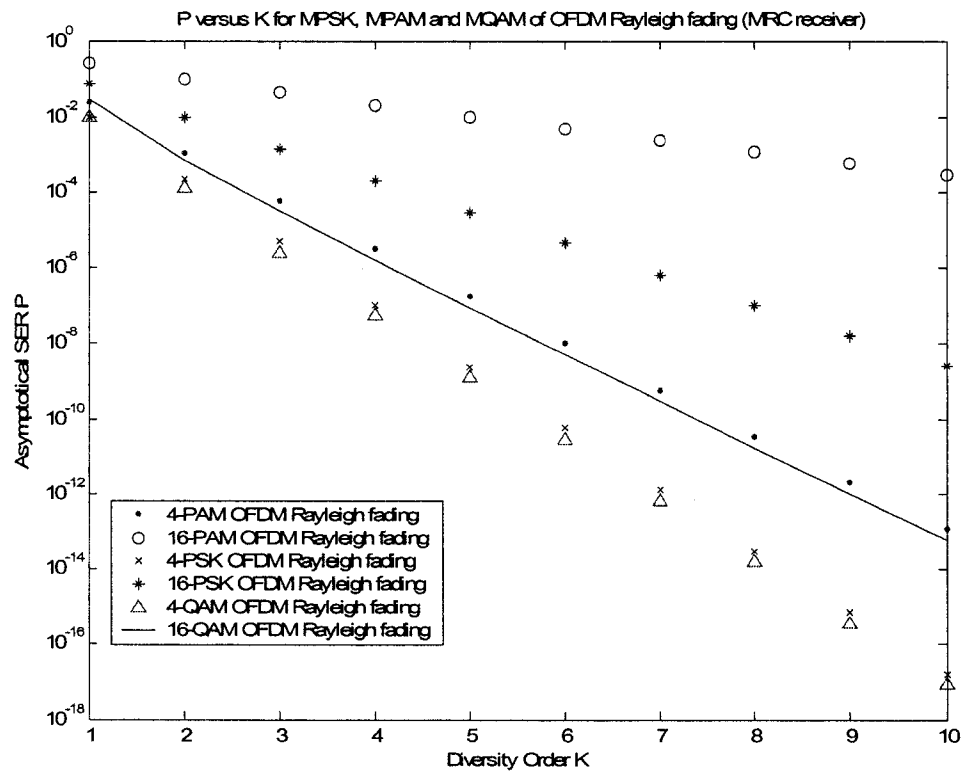OFDM Rician fading with MRC and EGC receiver

72

Figure 4.4 Asymptotical SER vs diversity order for MPSK, MPAM and MQAM of OFDM Rayleigh fading with MRC receiver
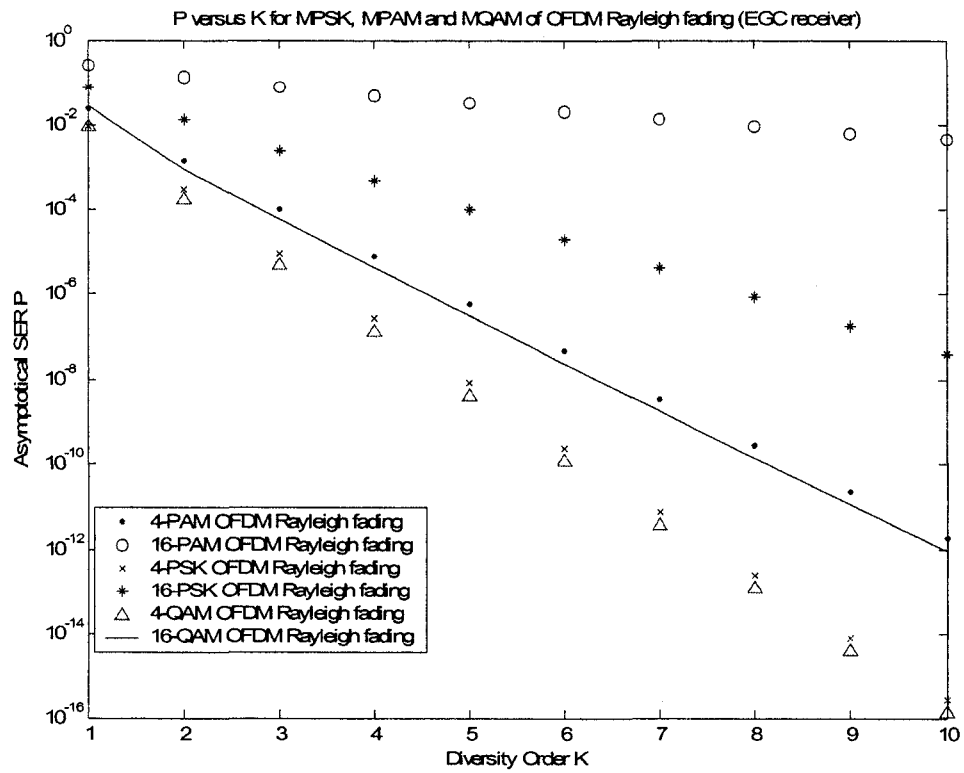
73

Figure 4.5 Asymptotical SER vs diversity order for MPSK, MPAM and MQAM of
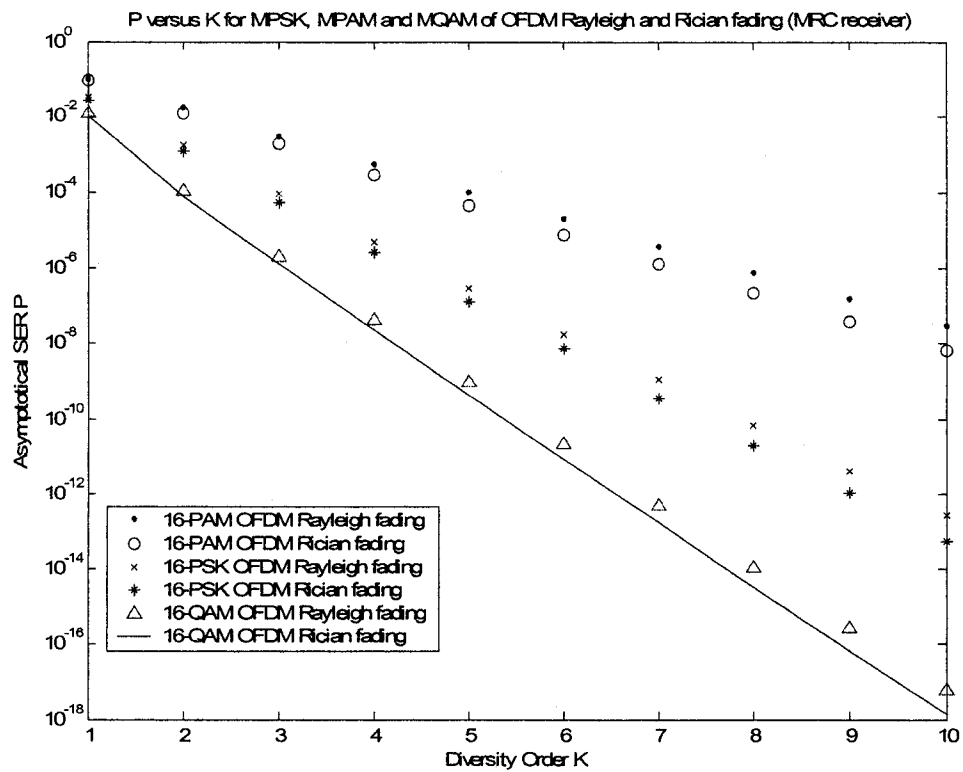OFDM Rayleigh fading with EGC receiver

74

Figure 4.6 Asymptotical SER vs diversity order for MPSK, MPAM and MQAM of OFDM Rayleigh and Rician fading with MRC receiver
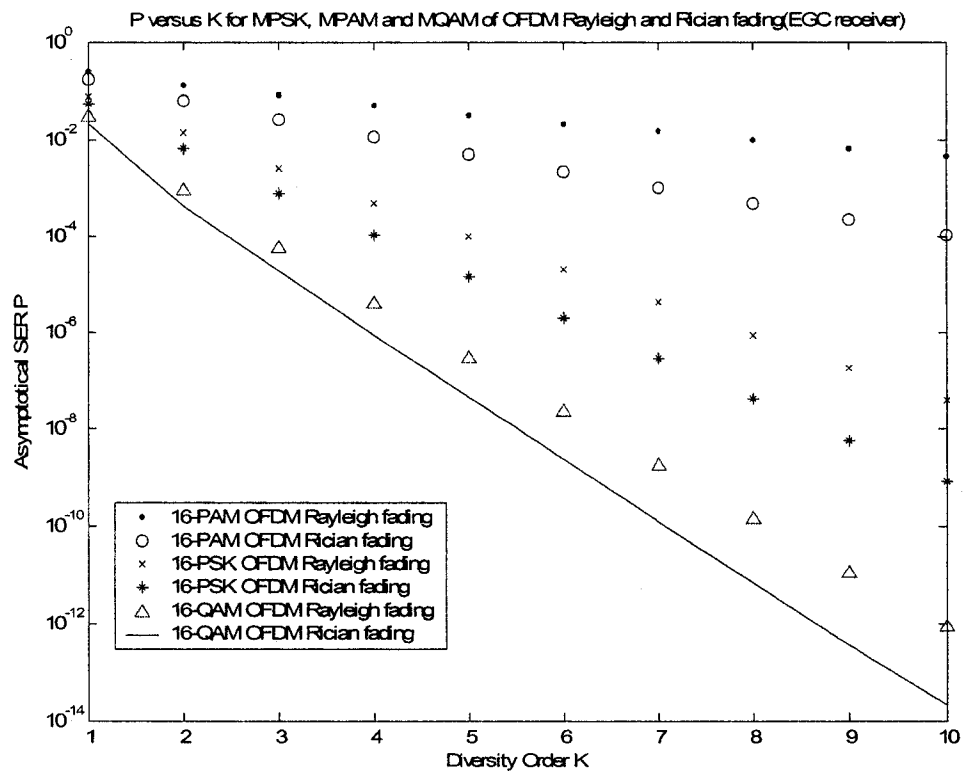
75

Figure 4.7 Asymptotical SER vs diversity order for MPSK, MPAM and MQAM of OFDM Rayleigh and Rician fading with EGC receiver
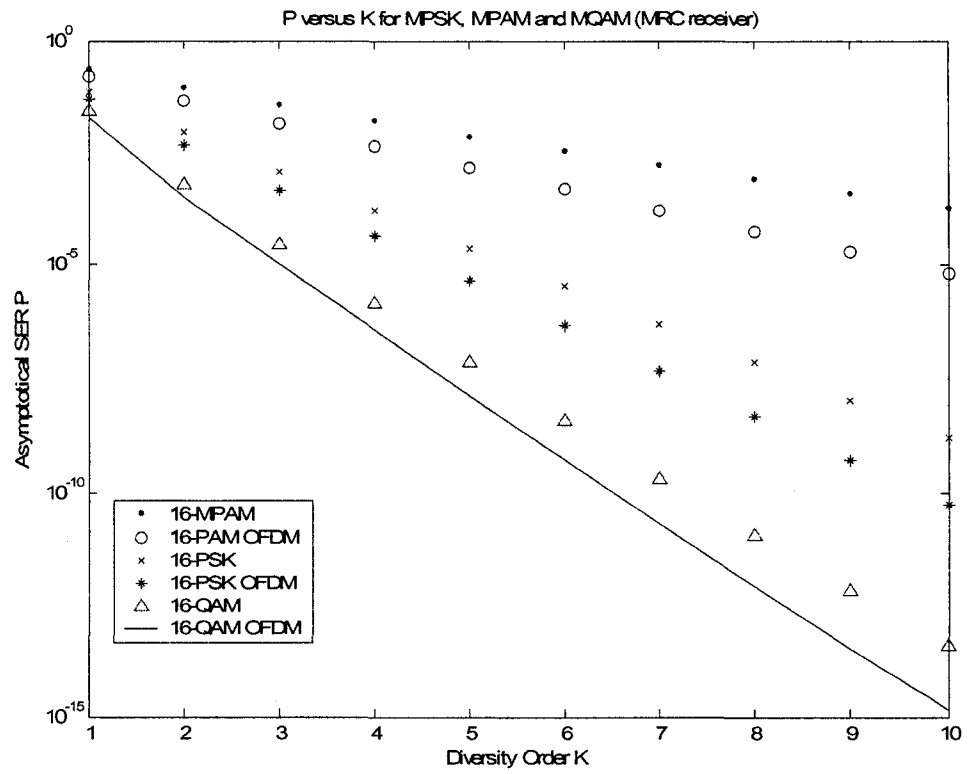
76

Figure 4.8 Asymptotical SER vs diversity order for MPSK, MPAM and MQAM of single carrier and OFDM with MRC receiver
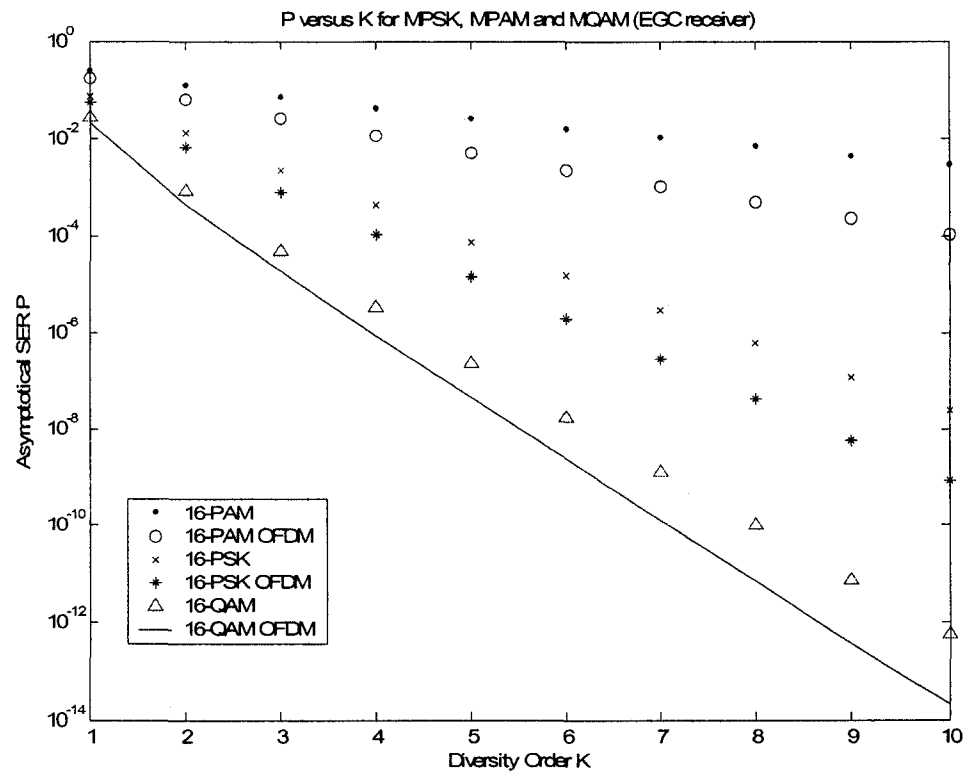
77

Figure 4.9 Asymptotical SER vs diversity order for MPSK, MPAM and MQAM of single carrier and OFDM with EGC receiver

78

# Chapter 5

# Conclusion and Future Study

The error rate performance of M-ary signals on multipath Rician fading diversity channels has been discussed. The exact error rate expressions are too complex. Therefore the asymptotic error rate at high average SNR's is considered. First we consider the asymptotic performance of single-carrier M-ary signals on multipath Rician fading diversity channels. A general theorem for the asymptotic error rate of general diversity receivers over multipath Rician fading has been derived, and two other theorems have been derived for the special cases where the conditional error probability is a function of the sum of the received SNR's or the sum of normalized received amplitudes, which correspond to the cases using MRC and EGC receivers, respectively. Then we consider the asymptotic performance of OFDM M-ary signals on multipath Rician fading diversity channels.

In the current study of OFDM error rate, we consider each subcarrier separately and do not take the cross-correlation between different subcarriers into consideration. In addition, no interference is included in the discussion. In the future study, the effect of the subcarrier cross-correlation and interference on OFDM M-ary signal error rate performance will be studied.

# References

[1] Hisham S. Abdel-Ghaffar and Subbarayan Pasupathy "Asymptotical performance of M-ary and binary signals over multipath/multichannel Rayleigh and Rician fading" IEEE Transactions on Communications, vol.43 no.11, pp.2721-2731, Nov. 1995

[2] John G. Proakis and Masoud Salehi *Fundamenals of Communication Systems* Pearson Prentice Hall, 2005

[3] John G. Proakis *Digital Communications* New York: McGraw Hill, 1995

[4] J. W. Craig "A new simple and exact result for calculating the probability of error for two-dimensional signal constellations" Proceedings of the IEEE MILCOM Conf., 1991, pp.571-575

[5] Theodore S Rappaport *Wireless Communications: Principle and Practice* Institute of Electrical & Electronics Engineers, 1995

[6] W. C. Lindsey "Error probabilities for Rician fading multichannel reception of binary and N-ary signals" IEEE Transactions Information Theory , vol. IT-10, pp.339-350, Oct. 1964

[7] D. G. Brennan "Linear diversity combining techniques" Proceedings of the IRE, vol. 47, pp.1075-1102, June. 1959

[8] M. Schwartz, W. R. Benett, and S. Stein *Communications Systems and Techniques* New York: McGraw Hill, 1966

[9] Ramjee Prasad *OFDM Wireless Communications Systems* Artech House Inc, 2004

[10] Andrea Goldsmith *Wireless Communications* Cambridge University Press, 1995

[11] Mohamed-Slim Alouini and Andrea J. Goldsmith "A unified approach for calculating error rates of linearly modulated signals over generalized fading channels" IEEE Transactions on Communications, vol.47 no.9, pp.1324-1334, Nov. 1999

[12] M. K. Simon and D. Divsalar "Some new twists to problems involving the Gaussian probability integral" IEEE Transactions on Communications, vol.46, pp.200-210, Feb. 1998

[13] I. S. Gradsteyn and I. M. Ryzhik *Table of Integrals, Series and Products* New York: Academic, 1980

[14] Z. Du, J. Cheng and N. C. Beaulieu "Accurate error-rate performance analysis of OFDM on frequency-selective Nakagaami-m fading channels" IEEE Transactions on Communications, vol.54, no. 2, pp.319-328, Feb. 2006

[15] J.D Parsons *The Mobile Radio Propagation Channel* New York: John Wiley &Sons Ltd, 2000